



GEOLOGICAL SURVEY OF WESTERN AUSTRALIA

Record 2001/15

GEOLOGY OF THE WESTERN YILGARN CRATON AND LEEUWIN COMPLEX, WESTERN AUSTRALIA — A FIELD GUIDE

by

S. A. Wilde¹ and D. R. Nelson²

¹ Curtin University of Technology, Western Australia

² Geological Survey of Western Australia

Perth 2001

MINISTER FOR STATE DEVELOPMENT
Hon. Clive Brown MLA

DIRECTOR GENERAL
DEPARTMENT OF MINERAL AND PETROLEUM RESOURCES
Jim Limerick

DIRECTOR, GEOLOGICAL SURVEY OF WESTERN AUSTRALIA
Tim Griffin

Notice to users of this guide:

This field guide is one of a series published by the Geological Survey of Western Australia (GSWA) for excursions conducted as part of the 4th International Archaean Symposium, held in Perth on 24–28 September 2001. Authorship of these guides included contributors from AGSO, CSIRO, tertiary academic institutions, and mineral exploration companies, as well as GSWA. Editing of manuscripts was restricted to bringing them into GSWA house style. The scientific content of each guide, and the drafting of the figures, was the responsibility of the authors.

REFERENCE

The recommended reference for this publication is:

WILDE, S. A., and NELSON, D. R., 2001, Geology of the western Yilgarn Craton and Leeuwin Complex, Western Australia — a field guide: Western Australia Geological Survey, Record 2001/15, 41p.

National Library of Australia Card Number and ISBN 0 7307 5703 X

Grid references in this publication refer to the Australian Geodetic Datum 1984 (AGD84). Locations mentioned in the text are referenced using Australian Map Grid (AMG) coordinates, Zone 50. All locations are quoted to at least the nearest 100 m.

Printed by The Digital Document Company (W.A.) Pty Ltd, Perth, Western Australia

Published 2001 by Geological Survey of Western Australia

Copies available from:

Information Centre
Department of Mineral and Petroleum Resources
100 Plain Street
EAST PERTH, WESTERN AUSTRALIA 6004
Telephone: (08) 9222 3459 Facsimile: (08) 9222 3444

This and other publications of the Geological Survey of Western Australia are available online through dme.bookshop at www.dme.wa.gov.au

Contents

Introduction	1
Geological setting	1
Overview of the main crustal components along the southwestern margin of Australia	1
Yilgarn Craton	1
Darling Mobile Belt	4
Orogenic activity	4
Post-orogenic events	5
Leeuwin Complex	6
Perth Basin	8
Northern Perth Basin	8
Southern Perth Basin	9
Geological evolution of southwestern Australia	9
Excursion localities	13
Day 1: Western margin of the Yilgarn Craton	13
Regional geology	13
Cardup Group	13
Balingup Metamorphic Belt	13
Granitic rocks of the southwestern Yilgarn Craton	14
Migmatite	15
Locality 1: Cardup Group unconformity	15
Locality 2: Migmatite, Jarrahdale Road	16
Locality 3: Logue Brook Granite, Logue Brook Dam	16
Locality 4: Gibraltar Quartz Monzonite	17
Locality 5: Balingup Metamorphic Belt, granofels	17
Days 2 and 3: The Leeuwin Complex	17
Regional geology	18
Geochemistry of the Leeuwin Complex	18
Previous geochronology	24
Geological evolution of the Leeuwin Complex	24
Locality 6: Pegmatite-banded granite gneiss, leucogabbro, and amphibolite, Skippy Rock	26
Locality 7: Anorthosite, Cape Leeuwin – Skippy Rock roads	26
Locality 8: Hornblende granite gneiss, Sarge Bay	26
Locality 9: Hornblende granite gneiss, Cape Leeuwin	27
Locality 10: Granite gneiss, Cosy Corner	28
Locality 11: Garnet–biotite–quartz–feldspar augen gneiss, Isaacs Rock	29
Locality 12: Biotite–hornblende monzogranite dyke, Gracetown	32
Locality 13: Hornblende–biotite granite gneiss, Cowaramup Bay North	33
Locality 14: Hornblende–biotite granite gneiss, Canal Rocks North	34
Locality 15: Aegirine–augite–quartz syenite gneiss, Gannet Rock	35
Locality 16: Bunker Bay	36
Locality 17: Bunbury Basalt	37
Acknowledgements	37
References	38

Figures

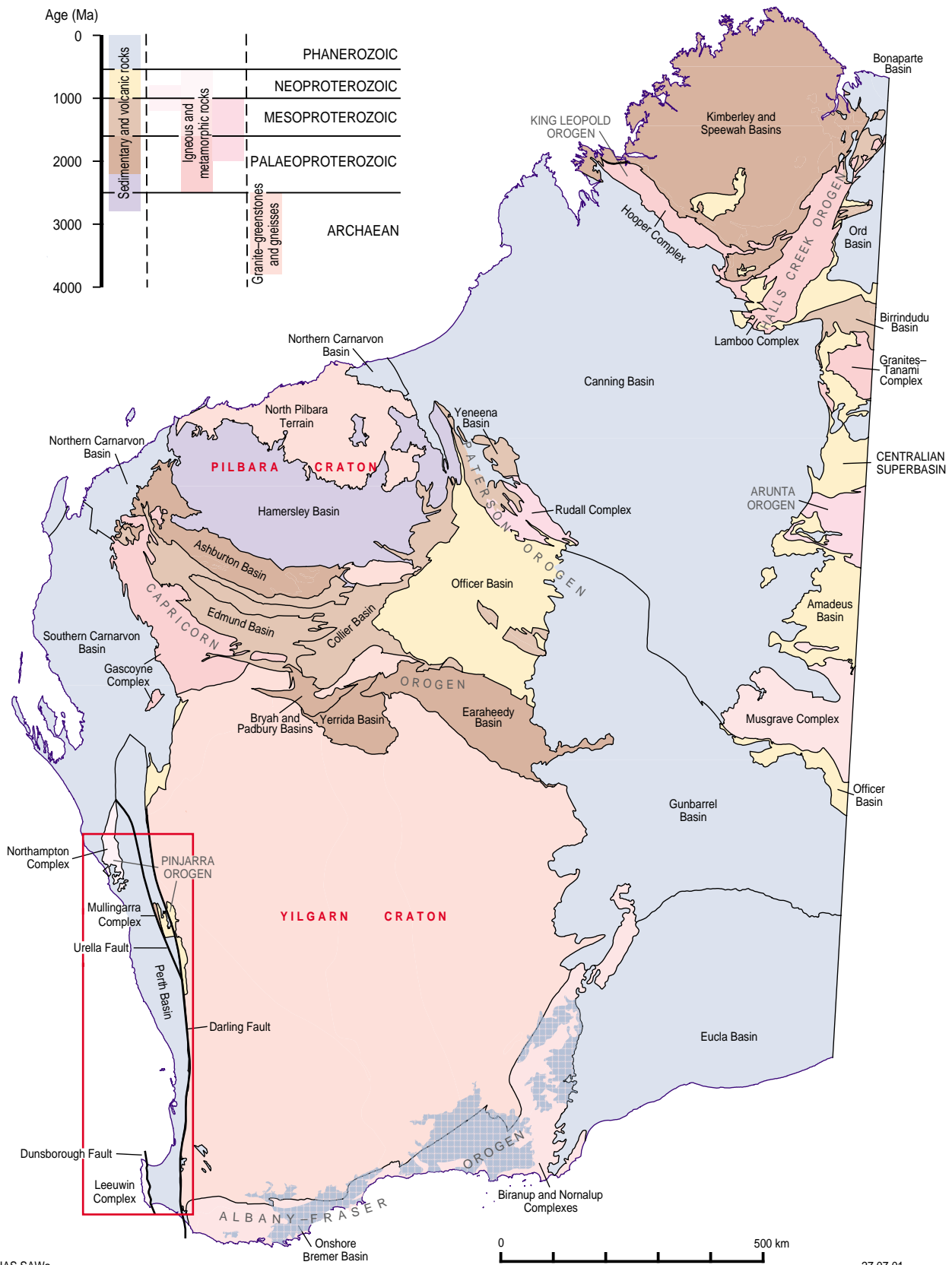
1. Geological map of the southwestern Yilgarn Craton, showing location of terrane boundaries	3
2. Generalized geological map of the Leeuwin Complex, showing the distribution of main rock types	7
3. Position of major rifts affecting East Gondwana at the time of breakup approximately 132 million years ago	11
4. Shand $\text{Al}_2\text{O}_3/(\text{Na}_2\text{O}+\text{K}_2\text{O})-\text{Al}_2\text{O}_3/(\text{CaO}+\text{Na}_2\text{O}+\text{K}_2\text{O})$ (molecular values) diagram showing alkalinity index of the Leeuwin granitoids	20
5. Chondrite-normalized rare earth-element diagrams for granitoid rocks from the Leeuwin Complex	21
6. Chondrite-normalized rare earth-element plot for samples from the Leeuwin Complex	22
7. The de la Roche diagram of Batchelor and Bowden (1985) indicating that the Leeuwin Complex samples of Wilde and Murphy (1990) and Nelson (1995) plot mainly in the ‘anorogenic’ field	23
8. Concordia diagram for 112132: granite gneiss, Cape Leeuwin lighthouse road	27
9. Concordia diagram for 112131: granite gneiss, Cape Leeuwin lighthouse	28
10. Concordia diagram for 112134: granite gneiss, Cosy Corner	29
11. Concordia diagram for 112135: augen gneiss, Redgate Beach	30
12. Concordia diagram for 112136: augen gneiss, Redgate Beach	31
13. Concordia diagram for 112140: monzogranite dyke, Gracetown	33

14.	Concordia diagram for 112143: monzogranite gneiss, Cowaramup Bay North	34
15.	Concordia diagram for 112144A: monzogranite gneiss, Canal Rocks North	35
16.	Concordia diagram for 112145: gneiss, Gannet Rock	36

Tables

1.	Geochemical data for selected rocks from the Leeuwin Complex	19
2.	Summary of the geological history of the Leeuwin Complex	25

Record 2001/15
Western Yilgarn and Leeuwin Complex Excursion



Geology of the western Yilgarn Craton and Leeuwin Complex, Western Australia — a field guide

by

S. A. Wilde¹ and D. R. Nelson²

Introduction

The aim of this excursion is to examine the evolution of the western margin of Australia from the Archaean to the present-day (Frontispiece). This will be achieved by visiting the southwestern part of the State, concentrating on key localities identified along the Darling Scarp and in the Leeuwin Complex. In order that these outcrops may be appreciated within their regional context, an overview of the geological evolution of southwestern Australia is also provided. This is based largely on the recent reviews by Wilde et al. (1996), Wilde (2000), and the work of Nelson (1995) on the Leeuwin Complex.

Geological setting

Overview of the main crustal components along the southwestern margin of Australia

The southwestern portion of Western Australia is composed of three main crustal entities: the Yilgarn Craton, Darling Mobile Belt, and Perth Basin. The term Darling Mobile Belt is used in preference to the 'Pinjarra Orogen' of Myers (1990) when referring to the western margin of the Australian continent, as this region has experienced a protracted history extending from the Middle Archaean and involving a number of orogenic episodes, the details of which are still poorly understood.

Yilgarn Craton

The Archaean Yilgarn Craton was cratonized approximately 2.6 billion years ago by the emplacement of extensive granitoids into pre-existing greenstone and high-grade gneissic belts (Gee et al., 1981). The original view of Gee et al. (1981) was that the Yilgarn Craton formed a major sialic block on which ensialic greenstone sequences developed. The identification of older inherited zircons within the greenstone sequences in the eastern part of the Yilgarn Craton by sensitive high-resolution ion microprobe (SHRIMP) studies (Compston et al., 1985; Campbell and Hill, 1988) appeared to substantiate this view of an older granitic basement to the greenstones. Alternatively,

¹ Curtin University of Technology, P.O. Box U 1987, Perth, W.A. 6845

² Geological Survey of Western Australia, 100 Plain Street, East Perth, W.A. 6004

Myers (1993) has argued for terrane accretion in all Precambrian regions of Western Australia, including the Yilgarn Craton where a number of discrete terranes have been identified within the northern and eastern portions of the craton. This approach has more recently been extended into the southwestern Yilgarn Craton (Wilde et al., 1996), based on new U–Pb zircon data and evidence from a deep-crustal geophysical survey.

When seismic, gravity, and ground-magnetic data obtained along a geophysical traverse line at New Norcia (Middleton et al., 1995) are extrapolated southward and constrained by regional geological, geochronological, and geophysical datasets, it is possible to delimit the main crustal components in the southwestern Yilgarn Craton. This has led to the recognition of three discrete terranes (Fig. 1) that, from west to east, are identified as the Balingup, Boddington, and Lake Grace Terranes (Wilde et al., 1996).

The Balingup Terrane (Fig. 1) is the one most pertinent to the present field excursion and consists of a narrow, north-trending zone delimited to the west by the Darling Fault and less precisely defined in the east by intrusive granitoids. The terrane consists of the Balingup and Chittering Metamorphic Belts (Fig. 1), which are characterized by turbiditic metasedimentary rocks and intensely deformed orthogneisses (Wilde, 1980). The age of sedimentation is not constrained; the only data being Sm–Nd model ages (Fletcher et al., 1985) suggesting that the precursors of the Balingup belt were formed between 3.07 and 2.83 Ga and for the Chittering belt at c. 2.89 Ga (Wilde, 1990).

The sequences were metamorphosed under medium-pressure, amphibolite-facies Barrovian conditions, with the development of kyanite, sillimanite, and staurolite in metapelites. A Rb–Sr isochron age of c. 2838 Ma from near Bridgetown (D. A. Nieuwland, quoted in Wilde, 1980) provides a possible constraint on the timing of metamorphism in the Balingup Metamorphic Belt. There are no comparable data for the Chittering Metamorphic Belt.

More recent U–Pb SHRIMP dating of granitoids from the Balingup and Boddington Terranes (Nemchin and Pidgeon, 1997) has indicated that they have a complex history. Zircons from these granites contain 2690–2650 Ma cores that are interpreted as dating either the source rocks or various stages of isotopic resetting due to recrystallization and melting of the protolith. The cores are surrounded by oscillatory zoned rims with ages of 2648–2626 Ma, which are interpreted as resulting from extended crystallization of the granites. The youngest zircon ages of 2628–2616 Ma were obtained from unzoned to weakly zoned outer rims that transgress the earlier zircon structures and may be the result of corrosion and recrystallization during slow cooling of the magma.

Some Archaean granitoids associated with the Balingup Terrane are amongst the youngest in the Yilgarn Craton. An ion microprobe U–Pb–Th zircon study of the Logue Brook Granite, located east of Bunbury (Fig. 1), by Compston et al. (1986) established a crystallization age of 2612 ± 5 Ma. In the Greenbushes area south of Balingup (Fig. 1), the Cowan Brook Dam and Millstream Dam granitoids recorded ages of c. 2577 Ma, whereas the Greenbushes Pegmatite has an age of 2527 Ma (Partington et al., 1986). All these rocks have undergone ductile deformation, with portions of the Logue Brook Granite infolded with paragneisses of the Balingup belt (Wilde and Walker, 1982). The Greenbushes Pegmatite was emplaced synkinematically into a major sinistral shear zone under medium-pressure, amphibolite-facies conditions (Partington et al., 1986).

Segments of a once-extensive transcurrent shear zone, subparallel to the present Darling Fault, are well preserved along the western margin of the Yilgarn Craton. In the South West region, the zones are up to 10 km wide and mark the western margin of the Balingup Terrane. There is evidence of a westward increase in deformation converting Archaean porphyritic granitoids, such as the Logue Brook Granite, into augen gneiss, mylonite, and ultramylonite (Wilde, 1990). Intense ductile deformation was

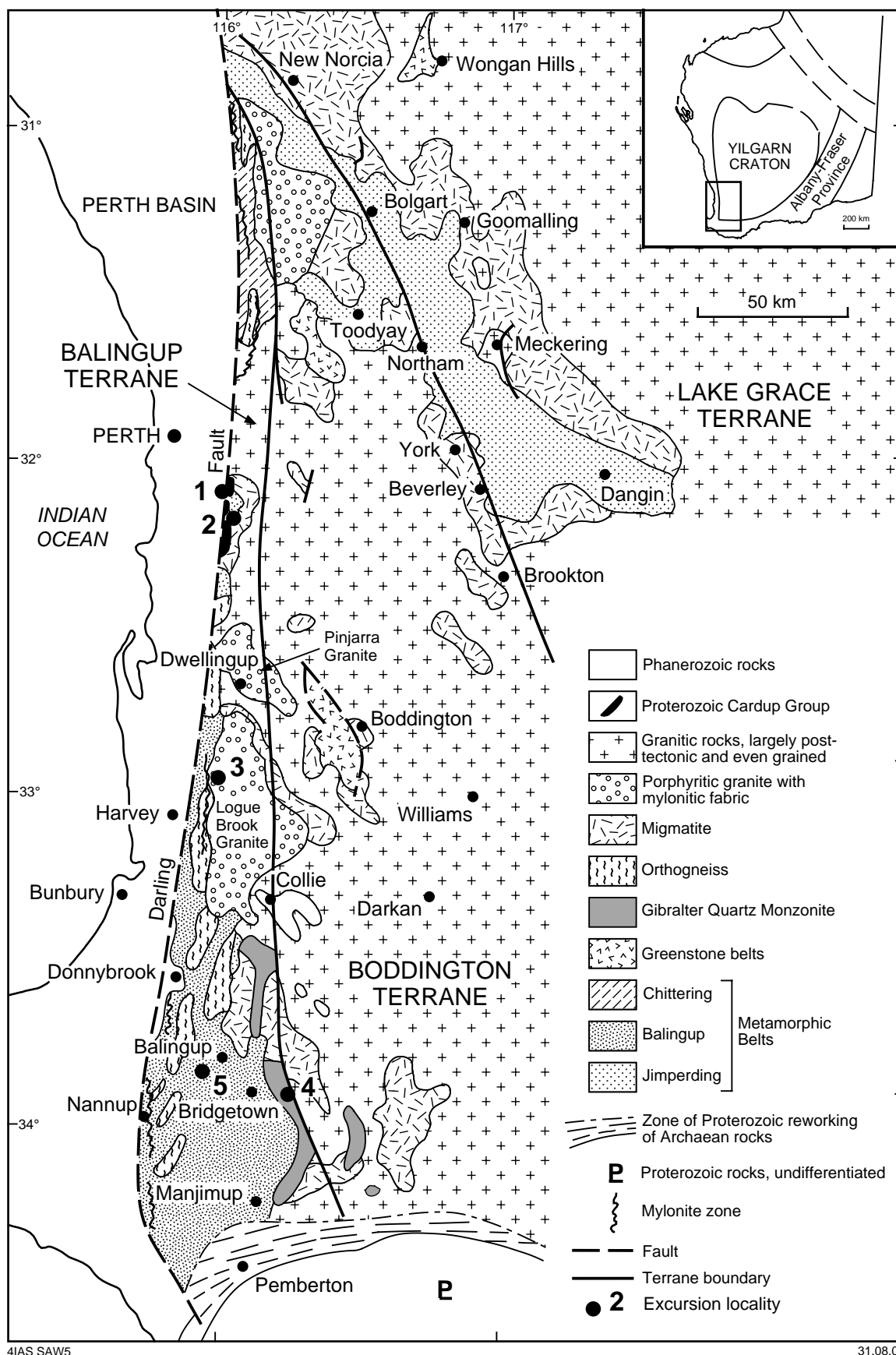


Figure 1. Geological map of the southwestern Yilgarn Craton, showing location of terrane boundaries and excursion localities (modified from Wilde, 1990)

associated with periodic movement along the Darling Fault Zone and commenced about 2577 million years ago (Blight et al., 1981), indicating that deformation took place soon after emplacement of the granite. Further evidence that the initial major deformation took place in the Archaean is provided by the fact that amphibolite-facies metamorphism, dated imprecisely by Arriens (1971) at 2606 ± 106 Ma using Rb–Sr techniques on orthogneiss at Pinjarra, post-dated ductile deformation in this area. Blight et al. (1981) argued that this major shear zone, referred to as the proto-Darling Fault, was periodically reactivated throughout the Proterozoic and acted as the locus for the Darling Fault during the Phanerozoic. The eastern boundary of the Balingup Terrane is defined in the extreme southeast by the Gibraltar Quartz Monzonite (Wilde and Walker, 1982, 1984), a metamorphic tectonite considered to have been emplaced during the peak of regional metamorphism. The Sm–Nd model age of 2.74 ± 0.09 Ga (Fletcher et al., 1983a) and Rb–Sr model age of c. 2828 Ma (Rosman et al., 1980) for this unit, although imprecise, are within error of D. A. Nieuwland's Rb–Sr isochron age (see Wilde, 1980) for the main metamorphic sequence.

By 2420 Ma, the Yilgarn Craton was assembled and was rigid enough to allow the emplacement of a major set of east–west-trending mafic dykes, known as the Widgemooltha Dyke Suite, that extend across the width of the craton (Fletcher et al., 1987; Nemchin and Pidgeon, 1997). Along the western margin, there was later reactivation associated with renewed movement along the Darling Fault (Bretan, 1985) and the development of the Darling Mobile Belt further to the west.

Darling Mobile Belt

Orogenic activity

High-temperature, medium-pressure Proterozoic orogens encircle the whole of the Yilgarn Craton (Gee, 1979; Myers et al., 1996). The Sm–Nd model ages are remarkably consistent (Fletcher et al., 1983a,b, 1985; McCulloch, 1987) and it has been suggested that they may have developed at the same time (Fletcher et al., 1985). However, since these ages are model dependant, the exact timing of mantle extraction is open to interpretation, since extensive mixing may have taken place. Using a depleted-mantle model, McCulloch (1987) recalculated the available data to define an age of 2.2 – 2.0 Ga for this event, whereas these ages become 2.0 – 1.8 Ga using a T_{CHUR} model (Fletcher et al., 1985). Although the possibility of mixing cannot be discounted, the consistency of the Sm–Nd results does favour major crustal addition during the Proterozoic. This age corresponds to a global collisional event and may reflect a period of crustal amalgamation during a supercontinent cycle (Zhao et al., 2000). The addition of material was originally considered to have occurred essentially in situ (Gee, 1979). However, more recent studies on the Albany–Fraser Orogen along the southwestern margin of the Yilgarn Craton (Beeson et al, 1988; Nelson et al, 1995) support extensive transport and accretion of exotic terranes, with some limited reworking of the Archaean Yilgarn Craton. Whatever the mechanism, the limited amount of Sm–Nd data can be interpreted to support either a broadly coeval extraction of material from the mantle in all mobile belts surrounding the Yilgarn Craton or else mixing between Archaean and younger Proterozoic components.

The mobile belt along the western margin of the Yilgarn Craton was originally referred to as the Darling Mobile Zone by Glikson and Lambert (1976), but was renamed the Pinjarra Orogen by Myers (1990). As stated above, this excursion guide uses the earlier name, since portions of several discrete orogens are incorporated in this belt (Wilde, 2000; Fitzsimons et al., 2001). The zone is poorly exposed and largely lies buried beneath the Perth Basin, with basement highs outcropping as the Northampton, Mullingar, and Leeuwin Complexes (Myers, 1990). In addition, some diamond drillcore is available from beneath the Perth Basin from petroleum exploration

wells (Fletcher et al., 1985; Fletcher and Libby, 1993). This core consists predominantly of garnetiferous granulites, gneisses, and migmatites. The gneisses of the Northampton Complex are largely of sedimentary origin (Peers, 1975; Bruguier et al., 1999) and underwent metamorphism prior to granite emplacement.

A Rb–Sr isochron age of 1018 ± 50 Ma was obtained by Compston and Arriens (1968) from granulites of the Northampton Complex, with the high initial $^{87}\text{Sr}/^{86}\text{Sr}$ ratio of 0.721 suggesting an earlier crustal history. A recent conventional and SHRIMP U–Pb study of zircon, monazite, titanite, and apatite by Bruguier et al. (1999) has indicated that metamorphism and initial deformation occurred at c. 1080 Ma and that a post- D_2 pegmatite has an age of 989 ± 2 Ma. Detrital zircons obtained from the paragneisses give a spread of ages back to 2043 Ma; significantly, Archaean zircons are absent. Populations grouped at 1.9 and 1.6 Ga could be consistent with a source to the northeast in the Capricorn Orogen, if the rocks are of local derivation and not part of an exotic terrane (Fitzsimons et al., 2001). Younger detrital zircons at 1450–1150 Ma suggest an additional source, possibly locally from within the Darling Mobile Zone, although this cannot be substantiated. It could thus be argued from the limited amount of available data that the Darling Mobile Zone underwent periodic reworking between 2.0 and 1.0 Ga. This is similar to the sequence of events recorded from the Albany–Fraser Orogen (Beeson et al., 1988; Nelson et al., 1995) along the southern margin of the Yilgarn Craton.

In a recent study of the northern part of the Mullingarra Complex, Cobb (2000) identified a little-deformed monzogranite with a Palaeoproterozoic age of 2181 ± 10 Ma. Overlying this, apparently in fault contact, is a strongly deformed metasedimentary sequence characterized by semi-pelitic rocks and quartzites, similar to those described from the nearby Northampton Complex (Bruguier et al., 1999). Detrital zircons record age populations at 1800–1600 Ma, 1450–1300 Ma, and 1200 Ma; zircons of Archaean age are extremely rare. This sequence underwent amphibolite-facies metamorphism that is imprecisely calculated at 1058 ± 83 Ma from thin overgrowths on detrital zircon grains; the youngest detrital grain was 1113 ± 26 Ma (Cobb et al., 2001). Similarities with the Northampton Complex in terms of lithologies, deformation and metamorphic histories, and available geochronology suggest that they form part of the same crustal block. The poor representation of Archaean detrital zircons in both the Northampton and Mullingarra Complexes, together with the lack of evidence for a metamorphic event at c. 1080 Ma in the adjacent Yilgarn Craton, may suggest that the two complexes were formed some distance from their present setting.

Post-orogenic events

Sedimentary successions that post-date orogenic activity (Low, 1975) were deposited on either side of the proto-Darling Fault, along much of the western margin of the Yilgarn Craton. Baxter and Lipple (1985) considered that there are two stratigraphically equivalent sequences of Proterozoic sediments developed north of Perth. On the Yilgarn Craton, the Moora Group forms a volcanic–clastic–carbonate shelf-platform sequence and includes the former Billeranga Group of Low (1975), from which an imprecise Rb–Sr isochron age of c. 1370 Ma was obtained by Compston and Arriens (1968) from the Morawa Lavas. West of the Darling Fault, the Yandanooka Group represents a thick basinal sequence of pelite and wacke that infills the Irwin Sub-Basin and is terminated to the west by the Urella Fault. Subsequent work has indicated that the Yandanooka Group should be considered as a basement inlier located within the Darling Mobile Belt (Hocking, 1994). It would thus appear that the proto-Darling Fault was active during the Mesoproterozoic, controlling the style of sedimentation along the western margin of the Yilgarn Craton. Rocks of the Mullingarra Complex (Frontispiece) are onlapped by the Yandanooka Group (Baxter and Lipple, 1985; Cobb, 2000), indicating

that sedimentation post-dated the high-grade metamorphic event that affected the complex at c. 1080 Ma (Bruguier et al., 1999; Cobb, 2000).

South of Perth, the Cardup Group (Low, 1975) forms a transgressive marine sequence exposed east of the Darling Fault, with the basal unconformity on Archaean granitoid now dipping 60° to the west (Wilde, 1980). Dolerite dykes have intruded the Cardup Group and it has been argued by Compston and Arriens (1968) that the age of deposition was between 735 and 550 Ma.

Although events in the Palaeoproterozoic and Mesoproterozoic appear to have been largely confined to the Darling Mobile Belt, there is evidence of limited igneous activity during the Neoproterozoic along the western margin of the Yilgarn Craton. Wilson et al. (1960) and Compston and Arriens (1968) reported a series of rather imprecise Rb–Sr whole-rock and mineral ages from pegmatites that range from c. 1073 to c. 500 Ma. There are also several suites of dolerite dykes with apparent ages ranging from Late Archaean to Neoproterozoic, based on palaeomagnetic and unpublished isotopic data (Giddings, 1976; Wingate and Giddings, 2000). The dolerites increase in abundance westward toward the Darling Fault, near which Rb–Sr ages of between 578 and 548 Ma have been obtained from sheared and metasomatized dyke margins (Compston and Arriens, 1968). There is also a corresponding westward decrease in the Rb–Sr biotite ages of Archaean granitoids (Libby and de Laeter, 1979; de Laeter and Libby, 1993; Libby et al., 1999), with the youngest ages of c. 500 Ma being found close to the Darling Fault. This resetting of the Rb–Sr isotopic system in biotites may be directly related to the emplacement of the dolerite dykes, reflect uplift of the western margin of the Yilgarn Craton, or signal the onset of tectonothermal activity within the adjacent Darling Mobile Belt.

Leeuwin Complex

The Leeuwin Complex has traditionally been grouped together with other Proterozoic basement rocks exposed along the western margin of Australia (Compston and Arriens, 1968; Harris, 1987) and was considered as part of the Pinjarra Orogen by Myers (1990). Along with Fitzsimons et al. (2001), we prefer to use the term Darling Mobile Belt for the whole group of basement complexes developed along the western margin of Australia, of which the Leeuwin Terrane is one (Wilde, 2000), since possibly three orogenic cycles may be recorded in rocks exposed in this zone. The Rb–Sr results obtained from Sugarloaf Rock near Cape Naturaliste (Fig. 2) by Compston and Arriens (1968) on whole-rock gneiss, pegmatite, and mineral separates define an isochron age of 655 ± 25 Ma. This was interpreted as the age of granulite-facies metamorphism and is broadly comparable with some mineral and pegmatite ages recorded along the western margin of the Yilgarn Craton.

The Sm–Nd chondritic model data of McCulloch (1987) and Fletcher et al. (1985) gave ages of c. 600 Ma. Fletcher and Libby (1993) recalculated these using a depleted-mantle model and values ranged from 1135 to 1083 Ma. Although the exact ages probably have no validity due to extensive mixing, they are nonetheless considerably younger than any so far obtained from sialic crust elsewhere in Western Australia, including adjacent areas of the Darling Mobile Belt, and thus indicate the presence of younger crust.

A Neoproterozoic to early Phanerozoic age for the Leeuwin Complex has been confirmed by the U–Pb zircon data of Wilde and Murphy (1990) and Nelson (1995). An initial single-grain U–Pb zircon study on the felsic gneisses gave the first indication that the rocks were Late Pan-African in age, with three zircon fractions of a granitic gneiss from near Cape Naturaliste (Fig. 2) giving concordant ages between 570 and

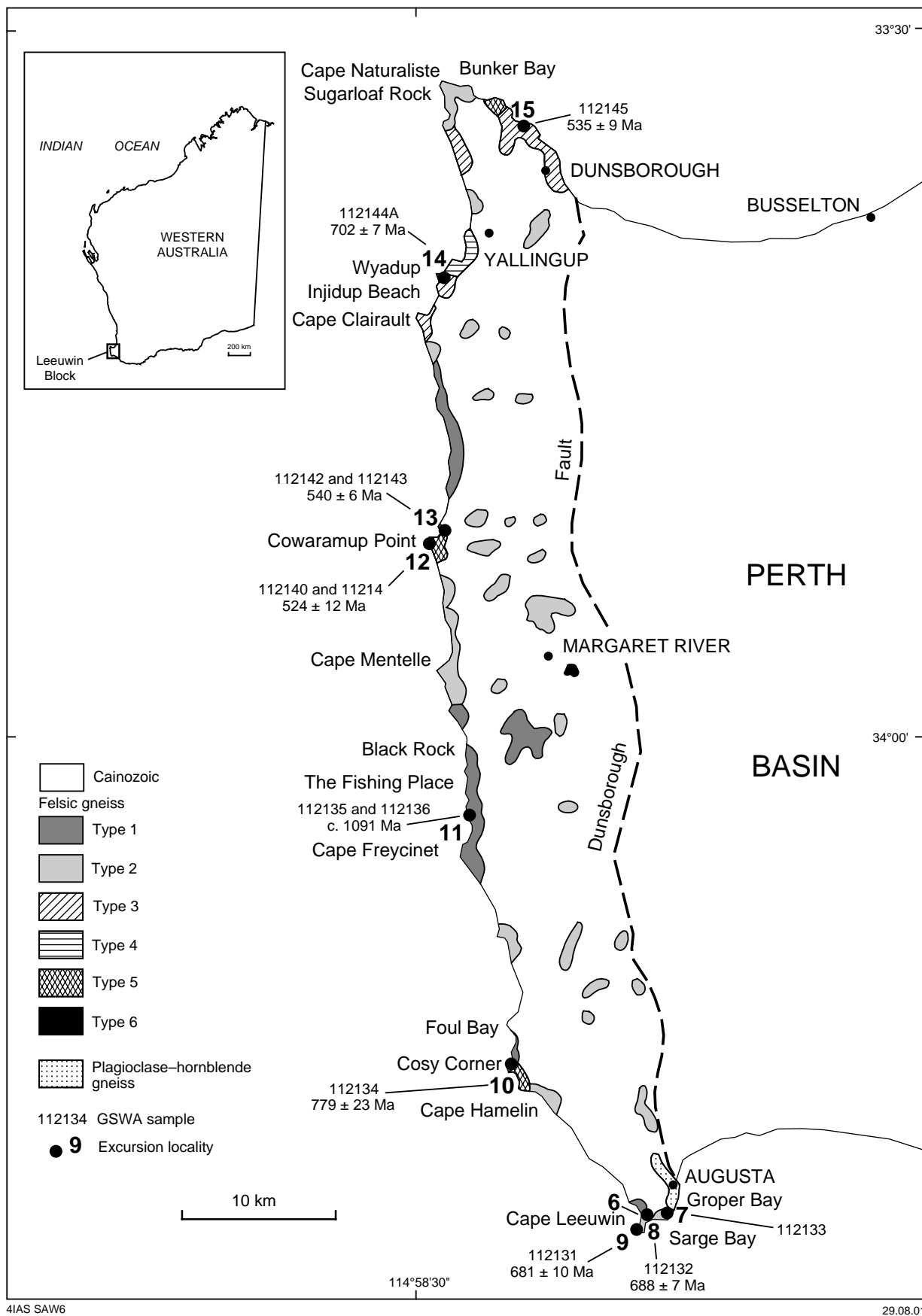


Figure 2. Generalized geological map of the Leeuwin Complex, showing the distribution of main rock types identified by Wilde and Murphy (1990). Excursion localities (numbered) and sites of GSWA samples are discussed in the text

550 Ma (Wilde and Murphy, 1990), which is younger than the Rb–Sr isochron age obtained by Compston and Arriens (1968) from Sugarloaf Rock. This apparent anomaly has been resolved by Nelson (1995), who determined the age of six gneisses using SHRIMP U–Pb zircon techniques. Nelson (1995) established that the felsic gneisses contain zircons that range in age from 779 to 524 Ma, with the older rocks pre-dating the peak of granulite-facies metamorphism that is considered to have occurred at c. 615 Ma. Nelson (1999) has recently identified gneisses with ages of c. 1090 Ma, which is the first evidence that rocks similar in age to the Northampton Complex are present in the Leeuwin Complex.

Myers (1994) informally subdivided the Leeuwin Complex into two major components: an older Cowaramup gneiss and a younger Hamelin granite. All rock types are granitoids and the favoured model (Wilde and Murphy, 1990; Wilde, 2000) is that these granitoids are of anorogenic, A-type affinity, and generated by intracrustal melting in a rift environment, with possibly a tonalite–granodiorite source (Creaser et al., 1991). Melt generation for A-type granites of this sort is likely to be at temperatures in excess of 830°C (Pitcher, 1993), or even greater than 900°C (Clemens et al., 1986). In the south of the complex near Cape Leeuwin, a gabbro–anorthosite is present (Wilde and Murphy, 1990; Myers, 1994) that Myers (1994) interpreted as the oldest component of the Cowaramup gneiss. Furthermore, he considered that a suite of dolerite dykes was intruded before the peak of metamorphism, which was coeval with his D₃ deformation event.

The available geochronological results establish that the Leeuwin Complex developed as a crustal entity during the Neoproterozoic – early Phanerozoic. It is one of the youngest discrete sialic crustal segments known in Western Australia and its age is similar to that of other Pan-African crustal segments widely distributed throughout Gondwanaland.

Perth Basin

The Phanerozoic evolution of the western margin of Australia has been documented by a number of workers (Falvey, 1972; Playford et al., 1976; Veevers and Cotterill, 1978; Fairbridge and Finkl, 1978; Powell et al., 1988; Veevers and Li, 1991; Veevers et al., 1991; Wilde, 2000).

The Darling Fault extends for almost 1000 km and marks the boundary between the Perth Basin to the east and the Yilgarn Craton to the west, with a normal downthrow of at least 10 km and possibly as much as 15 km to the west (Playford et al., 1976). It has developed subparallel to a major Precambrian shear zone, the proto-Darling Fault of Blight et al. (1981), and has controlled the evolution of the Perth Basin throughout the Phanerozoic (Fairbridge and Finkl, 1978). Playford et al. (1976) considered that it was probably active in the early Palaeozoic, but the greatest movement took place during the Middle Triassic to Early Cretaceous.

Northern Perth Basin

The Proterozoic basement complexes were formerly considered to form part of the Perth Basin (Playford et al., 1975, 1976) and, although subsequently reclassified by Hocking (1994), it is necessary to briefly comment on some aspects since these complexes clearly exerted control on the Phanerozoic development of the Perth Basin. The Mullingar Complex is bounded to the west by the Urella Fault and separated from the Darling Fault by the Irwin Sub-Basin (Playford et al., 1976) – Irwin Terrace of Hocking (1994). The Irwin Sub-Basin is filled by up to 10 km of Proterozoic sediments (Yandanooka Group), which are overlain by approximately 1.5 km of Permian strata that are exposed at the surface over a considerable area. This contrasts with the southern Perth Basin,

where the Permian sequence is buried by up to 10 km of younger strata (Wilde and Walker, 1982), thus supporting the view of Baxter and Lipple (1985) that post-Permian movement along the eastern margin of the Perth Basin was largely taken up in the north by the Urella Fault, which has an estimated vertical displacement of up to 9 km (Playford et al., 1975).

Southern Perth Basin

The Lower Cretaceous Bunbury Basalt and associated sediments extend eastward across the Darling Fault onto the Yilgarn Craton (Wilde and Walker, 1982, 1984). Frey et al. (1996) confirmed the existence of two lava types in the Bunbury Basalt, as was first proposed by Burgess (1978). The older suite (Casuarina type) has been dated at 130 ± 2 Ma and the younger suite (Gosselin type) at 123 ± 1 Ma by ^{40}Ar – ^{39}Ar methods (Frey et al., 1996). It has been suggested that the basalt was generated by the Kerguelen plume (Kent, 1991; Kent et al., 1992), which was believed to have been located beneath Eastern Gondwanaland prior to continental breakup. Furthermore, part of the Yarragadee Formation, which has yielded Oxfordian–Kimmeridgian microfossils, overlaps the Darling Fault at Fly Brook (Wilde and Walker, 1984). This indicates that major movement along the Darling Fault had ceased by the Middle Jurassic. Company aeromagnetic data (Chalmers, I., 1997, pers. comm.) indicate that the Bunbury Basalt can be traced across the Darling Fault along numerous palaeovalleys incised for up to 20 km eastward into the Yilgarn Craton. It is therefore evident that major movement on the Darling Fault had ceased by c. 175 Ma and therefore prior to the continental breakup of Greater India and Australia, which is considered to have occurred at c. 132 Ma (Powell et al., 1988; Veevers and Li, 1991; Veevers et al., 1991).

Geological evolution of southwestern Australia

From the above overview, coupled with more detailed information presented in the literature cited, it is possible to synthesize the geological development of the region.

Following stabilization of the Yilgarn Craton at c. 2.6 Ga, the evolution of the western margin of Australia was controlled by a major transcurrent shear zone (the proto-Darling Fault) and its Phanerozoic successor (the Darling Fault). Evidence indicates that the proto-Darling Fault was active in the Late Archaean, possibly during emplacement of the 2.6 Ga granitoids (Blight et al., 1981).

The shear zone later defined the eastern margin of a major mobile zone (the Darling Mobile Belt) that is one of a series of high-temperature–moderate-pressure terranes that enclose the Yilgarn Craton and have Sm–Nd T_{DM} model ages of c. 2.0 Ga (McCulloch, 1987). Distinct Palaeoproterozoic activity has only been identified in the Mullingar Complex, where Cobb (2000) has recognized a monzogranite with an age of 2181 ± 10 Ma. Geological activity during the Mesoproterozoic was largely confined to the mobile belt, and movement along the proto-Darling Fault shear zone may have controlled sedimentation of the Moora and Yandanooka Groups (Baxter and Lipple, 1985). However, this interpretation appears to conflict with the new U–Pb data of Bruguier et al., (1999) and Cobb (2000) for the Northampton and Mullingar Complexes, respectively. The Yandanooka Group has been considered the deep-water facies equivalent of the Moora Group, whose stable shelf facies was taken to mark the transition from a basinal to a platform environment that was controlled by a rifted continental margin (Baxter and Lipple, 1985). The Yandanooka Group onlaps the Mullingar Complex and its low metamorphic grade indicates that it was not present when high-grade metamorphism affected the underlying rocks of the Mullingar Complex. From the limited data available on the Mullingar Complex (Fletcher et al., 1985; Cobb, 2000), it appears to have a common evolution (including similar Sm–Nd

model ages) with the Northampton Complex, for which the new U–Pb geochronological data of Bruguier et al. (1999) indicate granulite-facies metamorphism at c. 1080 Ma. If the Yandanooka Group can indeed be equated with the Moora Group (Baxter and Lipple, 1985), for which an Rb–Sr age of c. 1370 Ma was reported for the Morawa Lavas by Compston and Arriens (1968), then clearly this interpretation is not in harmony with high-grade metamorphism of the Northampton and Mullingarra Complexes approximately 300 million years after deposition and eruption of these sequences. Further investigations are required to resolve this important problem in order to constrain the onset of rifting along the western margin of Australia; including work on the Cardup Group, which occupies a similar position to the Moora Group in the vicinity of Perth.

There is limited evidence to suggest that the Darling Mobile Belt was sporadically reworked over a period of at least one billion years. The Northampton Complex records trough-facies sedimentation, followed by high-grade metamorphism, migmatization, and granitoid emplacement at c. 1080 Ma (Bruguier et al., 1999). The c. 990 Ma emplacement of post-tectonic pegmatite in the Northampton Complex (Bruguier et al., 1999) indicates that there was little or no deformation within the Northampton Complex after this time.

The tectonic style along the western margin of the Yilgarn Craton, following amalgamation of the Grenvillian-age components of the Darling Mobile Belt, can be explained in two ways. Wilde (2000) argued that there was a change during the Neoproterozoic from a shear- and thrust-dominated regime associated with accretion in the mobile belt, to an extensional rift environment with granitoid emplacement initiated at c. 780 Ma (Nelson, 2000). The alkali-rich granitoids of the Leeuwin Complex contain sodic pyroxene and arfvedsonite, and are typical of A-type granitoids that characterize anorogenic rift environments (Loiselle and Wones, 1979). This period corresponds closely with the known onset of rifting (at 750–700 Ma) between Australia – East Antarctica and Laurentia, which lay to the present southeast of Australia at this time (Dalziel, 1991), eventually leading to the breakup of Rodinia (Torsvik et al., 1996). Alternatively, Nelson (1995) favours development of the Leeuwin Complex as an exotic terrane, possibly associated with Antarctica, that was transposed northward by strike-slip movement adjacent to the western margin of the Yilgarn Craton. This view has also been supported by Fitzsimons et al. (2001).

Whatever the location, it seems likely that granitoids were emplaced throughout the complex from c. 1100 Ma until c. 615 Ma, when strong deformation and granulite-facies metamorphism affected the Leeuwin granitoids (Myers, 1994). Pressure conditions were low (Wilde and Murphy, 1990) and it is postulated that granulite-facies metamorphism may have resulted from mantle-plume activity and underplating of hot mafic magmas, rather than crustal thickening. This is consistent with the geochemical and isotopic data from the Leeuwin Complex (Wilde and Murphy, 1990; Nelson, 1995; Wilde, 2000) that indicates high-temperature, intracontinental melting of a tonalite–granodiorite source to produce the A-type granitoids.

The Darling Fault controlled the development of the Perth Basin along the western margin of the Yilgarn Craton throughout the Phanerozoic, and developed subparallel to an original Archaean shear zone. Movement may have commenced in the Late Ordovician in the northern Perth Basin (Playford et al., 1975), but does not appear to have taken place in the south until the Early Permian (Wilde, 1981). Downthrow along the Darling Fault resulted in the formation of the ‘Westralian Aulacogen’ (Fairbridge and Finkl, 1978), a rift valley separating the Yilgarn Craton from the Leeuwin Complex (and its northern extensions), with Greater India located further to the west. Veevers and Cotterill (1978) postulated the existence of two rift systems along the western coast of Australia at this time (Fig. 3). The inner arm was considered to be the Perth Basin and was confined in the south by the Darling and Dunsborough Fault Systems. However,

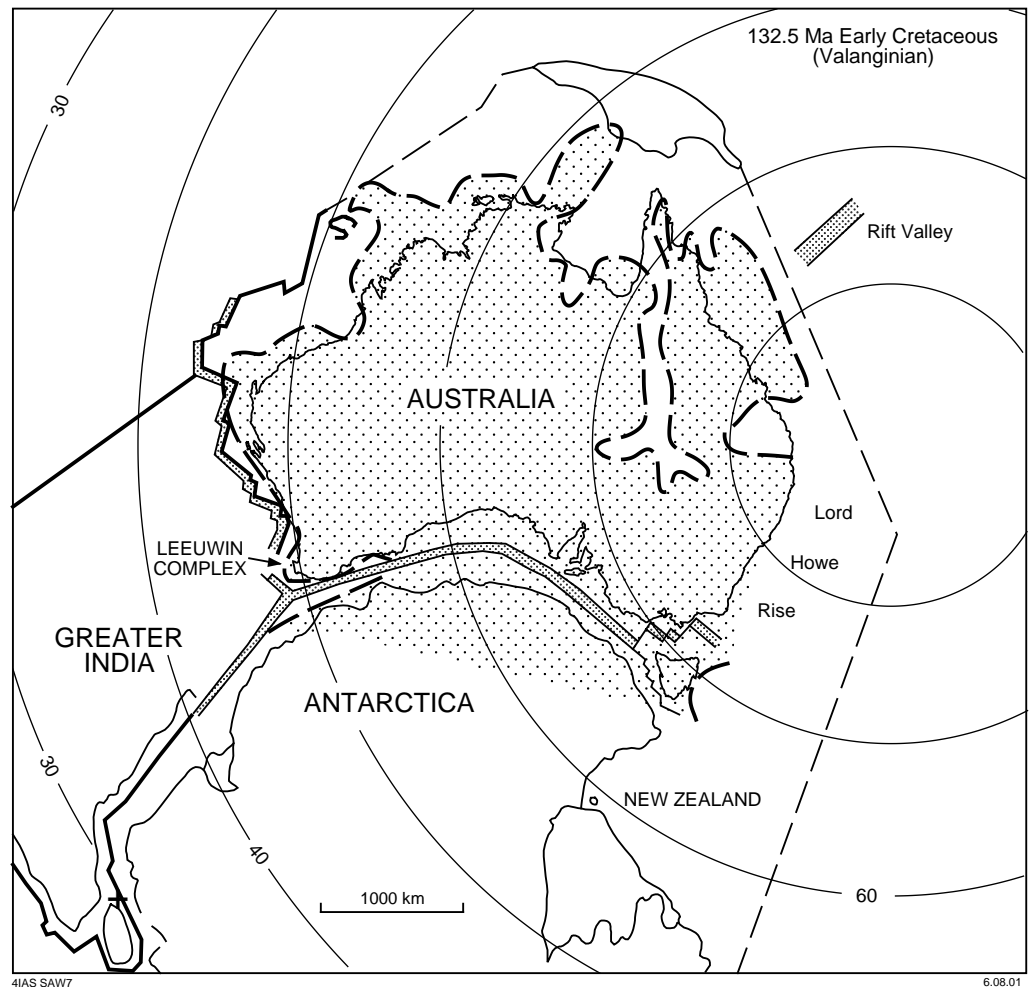


Figure 3. Position of major rifts affecting East Gondwana at the time of breakup approximately 132 million years ago. Circles represent palaeolatitudes around a pole centred off eastern Australia (modified from Veevers et al., 1991 and Wilde, 2000)

the sealing of the former by the Permian (in the north) and by the Middle Jurassic (in the south) meant that breakup did not take place along the inner rift system. Instead, Early Cretaceous plate divergence took place along the 'outer' arm of the rift system (Fig. 3), which is considered to have contained more abundant volcanic rocks and to have had a higher heat flow (Veevers, 1984).

It is plausible that the eastern boundary of the 'outer' rift was in fact the faulted western margin of the Late Pan-African granulite terrain, now represented in Western Australia by the Leeuwin Complex (Wilde, 2000). Breakup occurred at c. 132 Ma (Powell et al., 1988) and was followed shortly after by eruption of the Bunbury Basalt in two pulses at 130 and 123 Ma (Frey et al., 1996). Kent (1991) has suggested that the Bunbury Basalt may be a reflection of the Kerguelen plume and that this was possibly a hot spot beneath Eastern Gondwanaland prior to continental breakup. Doubt has been cast on this view, with the reconstruction of Müller et al. (1993) suggesting that the Bunbury Basalt was erupted 1000 km from the plume. The geochemical and isotopic data of Frey et al. (1996), whilst consistent with a genetic relationship to the plume in having similar Sr and Nd ratios to younger lavas from the Kerguelen Archipelago, nonetheless indicate that they are older than the oldest known ages of c. 115–110 Ma from the Kerguelen Plateau (Whitechurch et al. 1992; Pringle et al.,

1994). Frey et al. (1996) concluded that any similarities between the Bunbury Basalt and the Kerguelen lavas may be fortuitous. The fact that the Kerguelen Plateau lavas post-date continental breakup by more than 15 million years indicates that the plume did not have a major influence on plate divergence.

Following breakup, the western edge of Australia has acted as a passive trailing margin. Less than one kilometre of sediment has built up over the Perth Basin in the approximately 125 million years since the initiation of drift (Playford et al., 1976).

Excursion localities

Day 1: Western margin of the Yilgarn Craton

Regional geology

The excursion will visit localities within the Balingup Terrane, as defined in the preceding section. Specifically, the localities include Archaean granitoids and components of the Balingup Metamorphic Belt, as well as the overlying Proterozoic Cardup Group sediments (Wilde, 1980).

The area is dominated by the north-trending Darling Scarp, which is the eroded western margin of the exposed Yilgarn Craton, and is considered by some to be the surface expression of the Darling Fault. However, the fault lies between 1 and 3 km to the west of the scarp, hidden by sediments of the Perth Basin, and the scarp is strictly a marine erosion feature that reflects extended periods of both pre- and post-Cretaceous activity. Inland of the Darling Scarp lies the Darling Plateau, an ancient peneplain developed over the Yilgarn Craton, with an average elevation of 300 m. Archaean bedrock is capped by an extensive laterite profile that has been partially dissected by the present drainage. In the south near Bunbury, the expression of the Darling Scarp is more subdued, due in part to the presence of a second scarp (the Whicher Scarp) that splays off to the south-southwest. The area between the two scarps consists of laterite overlying Cretaceous sediments and is referred to as the Blackwood Plateau. This was once more extensive and extended to the north of Perth where it combined with the Dandaragan Plateau, which is similarly developed over Cretaceous sediments. It was the removal of this section that led to the enhancement of the Darling Scarp in this region. The Whicher Scarp is also a complex marine erosional feature, possibly developed during the Tertiary to Pleistocene. It contains distinct strandlines at elevations of 75–80 m and 45–50 m above sea level, with local heavy-mineral deposits. Beneath the Whicher Scarp in the south and the Darling Scarp to the north, lies the Swan Coastal Plain, which developed over Phanerozoic rocks of the Perth Basin. The plain ranges up to 60 m above sea level and consists of a complex interplay of piedmont fans, alluvial tracts, and more recent eolian dune systems. The underlying Perth Basin shallows southward, from approximately 15 km in thickness near Perth (Wilde and Low, 1978) to less than 6 km in the south (Wilde and Walker, 1984). The strata range in age from Early Permian to Middle Cretaceous.

Cardup Group

The Cardup Group (Low, 1975) is a prograding sequence of conglomerate, sandstone, siltstone, and shale that outcrops sporadically along the Darling Scarp over a distance of about 35 km, from Serpentine in the south to Maddington in the north (Fig. 1). The Cardup Group is considered to have been deposited in either the Mesoproterozoic or Neoproterozoic, although there is no precise isotopic data to more tightly constrain this age. It lies along the Darling Scarp in a similar position to the Moora Group, some 200 km to the north, which is generally considered to be Mesoproterozoic in age (Baxter and Lipple, 1985).

Balingup Metamorphic Belt

The Balingup Metamorphic Belt extends for over 200 km, from Pemberton in the south to the vicinity of Perth in the north (Wilde, 1980, 1990). It narrows from about 50 km maximum width in the south near Bridgetown to about 3 km in width in the north, where the belt is dismembered into isolated lenses by the intrusion of granitoids and the development of migmatite. The belt is truncated to the west by the Darling Fault

and to the east by the 100 km-long Gibraltar Quartz Monzonite, at least in the southern portion. Further north, the eastern boundary is obscured by laterite.

The Balingup Metamorphic Belt consists of an extensive sequence of quartz–feldspar–biotite(–garnet) gneiss interleaved with large areas of quartz–feldspar–biotite (–hornblende–garnet) granofels and thin units of quartzite, banded iron-formation (BIF), quartz–mica- and kyanite-bearing schist, calc-silicate gneiss, amphibolite, and ultramafic rocks, all cut by tectonically emplaced masses of orthogneiss. The hornblende–clinopyroxene–labradorite assemblage of fine-grained amphibolite, the diopside–epidote–plagioclase–microcline–titanite assemblage of calc-silicate gneiss, and the quartz–grunerite–magnetite(–garnet) assemblage of the BIF, together with the rare development of kyanite and staurolite in aluminous schists near Bridgetown, indicate medium-pressure Barrovian metamorphism.

Orthogneiss bodies make up approximately 30% of the belt and are chiefly derived from porphyritic granite (similar to the Logue Brook Granite) that is deformed, infolded, and in tectonic contact with the layered sequence. These bodies are elongated in a north-northeasterly trending direction and are commonly the core of anticlinal axes. Two earlier phases of folding can be identified in the layered sequence; the earliest is isoclinal, although large-scale structures have not been identified, and these are folded by more upright east–west-trending structures. Both the layered sequence and the orthogneiss are cut by extensive mylonitic shear zones. These shear zones increase in abundance, width, and intensity westward toward the Darling Fault.

Granitic rocks of the southwestern Yilgarn Craton

The granitic rocks along the western margin of the Yilgarn Craton have been grouped together into several batholiths, the largest of which is the ‘Darling Range Granite’ (Wilson, 1958; Wilde and Low, 1978). The lithologies range in composition from granodiorite, through monzogranite, to syenogranite, and this is commonly independent of textural changes. Locally, transgressive relations can be identified and fine-grained granodiorite is commonly the earliest phase.

There are three discrete batholiths of porphyritic granite in the Balingup Terrane, along the eastern boundaries of the Chittering and Balingup Metamorphic Belts and in close proximity to the craton margin (Fig. 1). Unlike the majority of granitoids in the southwestern Yilgarn Craton, which have undergone only minor, local recrystallization, these show evidence of intense deformation. Two of these, the Pinjarra and Logue Brook Granites (Fig. 1), are located adjacent to the Balingup Metamorphic Belt, where there is a general westward increase in the intensity of deformation, resulting in a progressive change from porphyritic granite to augen gneiss, mylonite, and ultramylonite (Blight et al., 1981). Subsequent recrystallization has resulted in local destruction of the mylonitic fabric, with the formation of layered gneisses. Metamorphic minerals have also locally overprinted the mylonitic fabric (Wilde and Low, 1978), indicating that deformation was pre- or synmetamorphic.

In the Balingup Metamorphic Belt, an ion microprobe U–Pb–Th zircon study of one of these porphyritic granite batholiths (the Logue Brook Granite located east of Bunbury; Fig. 1) was undertaken by Compston et al. (1986) and they established a crystallization age of 2612 ± 5 Ma. Blight et al. (1981) had previously determined a Rb–Sr age of 2577 ± 50 Ma for the Logue Brook Granite, which included mylonites and orthogneisses that were interpreted as deformed varieties of the granite; this younger age was considered to mark the timing of initial deformation along the proto-Darling Fault. In the Greenbushes area, south of Balingup (Fig. 1), c. 2577 Ma ages were recorded for the Cowan Brook Dam and Millstream Dam granitoids, whilst the Greenbushes Pegmatite has an age of 2527 Ma (Partington et al., 1986). All these rocks

have undergone ductile deformation, with portions of the Logue Brook Granite infolded with paragneisses of the Balingup belt (Wilde and Walker, 1982). The Greenbushes Pegmatite is a late-stage granitoid emplaced synkinematically into a major sinistral shear zone under medium-pressure, amphibolite-facies conditions (Partington et al., 1986). Pb–Pb whole-rock (Partington et al., 1986) and ion microprobe U–Pb zircon data (Partington, 1990) from granitoids in the Greenbushes area indicate magmatic activity equivalent in age or slightly younger than the Logue Brook Granite.

A distinctive, tectonized quartz monzonite (Gibraltar Quartz Monzonite) marks the eastern boundary of the Balingup Metamorphic Belt, and is present as a narrow, discontinuous zone for almost 100 km in length (Fig. 1). It is associated with migmatite and may have formed by deep-level partial melting of an amphibolite-bearing gneissic sequence in a high-temperature, anhydrous environment (Wilde and Walker, 1982). There are currently no U–Pb zircon data for the Gibraltar Quartz Monzonite, but a Sm–Nd model age of 2.74 ± 0.09 Ga (Fletcher et al., 1983a) and a Rb–Sr model age of c. 2828 Ma (Rosman et al., 1980), although not precise, are within error of D. A. Nieuwland's (see Wilde, 1980) Rb–Sr isochron age for metamorphism of gneisses within the Balingup Metamorphic Belt.

Migmatite

Migmatites, composed of earlier gneissic rocks intimately admixed with a later granitic component, form extensive areas in the southwestern part of the Yilgarn Craton. They principally occur along the margins of the Jimperding, Chittering, and Balingup Metamorphic Belts (Fig. 1), and much of the gneissic palaeosome was derived by reworking of the earlier metamorphic rocks. Some of the granitic neosomes appear to be derived by in situ partial melting of the gneisses, particularly along fold axes (Wilde and Low, 1978), although many are undoubtedly intrusive. There are also migmatites formed by late-stage emplacement of granite into older deformed granitoid.

The excursion localities are marked on Figure 1.

Locality 1: Cardup Group unconformity

The Cardup Group (Low, 1975) is a prograding sequence of conglomerate, sandstone, siltstone, and shale that outcrops sporadically along the Darling Scarp from Serpentine in the south to Maddington in the north (Fig. 1), a distance of about 35 km.

This disused quarry (AMG 407300E 6444400N) was the source of brickmaking shale and fed the old Orange Grove Brickworks; it has been abandoned since the late 1970s. It is the only outcrop where the Proterozoic Cardup Group can be seen to unconformably overlie Archaean granite.

In the eastern wall of the old quarry, the basal conglomerate of the Cardup Group has a general trend of $146/62^\circ\text{W}$, although the actual contact shows gentle undulations due to post-depositional tectonism. In the field, the contact is very distinct, with the basal Cardup Group marked by a 3 m-thick unit of pebble conglomerate and interlayered granulestone. In thin section, it is more difficult to identify the contact; the distinctive feature being the rounded nature of quartz pebbles in the conglomerate as opposed to the angular quartz in the granite. These features suggest that the underlying Archaean granite was extensively weathered prior to the marine transgression that resulted in deposition of the Cardup Group. The rounded quartz pebbles average 1 cm in diameter and are set in a matrix of angular quartz and feldspar. Thin layers of arkose and siltstone are also present and these predominate 3 m from the contact. A further 5 m up-sequence, the siltstones pass into pale, cream shale, which is the material that was quarried for bricks.

Locality 2: Migmatite, Jarrahdale Road

An old disused road-metal quarry is located in migmatite (AMG 407400E 6425900N). The chief rock type is a medium- to coarse-grained porphyritic monzogranite, with microcline megacrysts up to 4 cm long and enclosing small crystals of sericitized plagioclase. The rock has been converted to an augen gneiss with most crystal boundaries interlobate to amoeboid. The quartz is intensely strained and greenish biotite has recrystallized into clusters of small flakes that show a weak alignment that trends 157/44°SW. Veins of fine-grained monzogranite, some rich in epidote, crosscut the augen gneiss to constitute a migmatite. There are also later shear zones with abundant chlorite and epidote, and local pyrite. There are also areas where the gneissic fabric is more intense, with a foliation defined by mafic schlieren or streaked-out lenses of amphibolite.

Regionally, this migmatitic area is developed between undeformed even-grained and porphyritic granite to the east and layered gneissic rocks of the Balingup Metamorphic Belt to the west. It appears likely that the original porphyritic granite in this area was once part of the Pinjarra Batholith (a large porphyritic granite body to the south), but has been largely dismembered by deformation, recrystallization, and migmatization. Arriens (1971) obtained a Rb–Sr age of 2608 ± 106 Ma from augen gneisses of this type east of Pinjarra, and this may approximate the timing of deformation and metamorphism.

Locality 3: Logue Brook Granite, Logue Brook Dam

The Logue Brook Granite (Wilde and Low, 1978) is 900 km² in surface area and is one of three discrete batholiths of porphyritic granite that are present along the southwestern margin of the Yilgarn Craton (Fig.1). All are megacryst rich and have undergone ductile deformation that increases in intensity westward toward the Darling Fault.

The emplacement age of the Logue Brook Granite has been determined by Compston et al. (1986) at 2612 ± 5 Ma. The granite outcrops in several localities along the banks of Logue Brook Dam (AMG 403500E 6346400N). It contains tabular megacrysts of microcline, commonly more than 2 cm long, that are set in an allotriomorphic granular aggregate of microcline, albite–oligoclase, and quartz, with minor biotite that may be grouped locally into clusters. Even in the least deformed varieties, there has been some recrystallization of quartz into marginal subgrains and this increases markedly toward distinct mylonitic shear zones. The shear zones mostly trend 008° and are subparallel to the microcline alignment, which is probably of igneous origin. Veins of fine-grained granodiorite trend 140° through the granite and are also cut and offset by the shear zones, whose mylonitic fabric intensifies over a width of only a few centimetres. The centre of the shear zones consists of extremely fine-grained blastomylonite in which all traces of microcline megacrysts have been destroyed.

Based on evidence from here and other localities close to the Darling Scarp, it has been possible to reconstruct the deformation history of the Logue Brook Granite. The earliest preserved fabrics reveal conjugate shear zones with a dihedral angle close to 80°. Shears composed of fine-grained recrystallized quartz and mimetic biotite cut the corners off microcline megacrysts where they intersect. Increased deformation is marked by a closer spacing of the shear zones, with extensive recrystallization of quartz between the megacrysts. The next stage is one of flattening, marked by a distinct rounding of the ends of the original megacrysts and the development of augen. The final phase is accompanied by recrystallization, and results in an almost layer-parallel structure where biotite-rich bands alternate with layers rich in platy quartz derived by recrystallization of flattened quartz mosaics. This is accompanied by grain-size reduction and megacrysts

become both smaller and rarer. The centre of most shear zones consists of extremely fine-grained blastomylonite. On a regional scale, metamorphic recrystallization increases westward, and the result is a granitic gneiss with distinct alternation of biotite-rich and microcline-rich layers; no megacrysts have survived this deformation.

Locality 4: Gibraltar Quartz Monzonite

The Gibraltar Quartz Monzonite is exposed on either side of the track (AMG 433800E 6239500N) leading east from Bridgetown to Winnajup. It consists of microcline megacrysts set in a xenoblastic, granular groundmass of microcline, plagioclase, and quartz. Poikiloblastic hornblende encloses small crystals of quartz and plagioclase.

This rock unit defines the eastern margin of the Balingup Metamorphic Belt and is interleaved with migmatite at several localities. There is a fault between the metamorphic belt and granitoids to the east in this area. A number of en echelon faults can be detected on aerial photographs and one accounts for a north-trending section of the Blackwood River. Further north, the outcrop is poor and the contact is not seen. The Gibraltar Quartz Monzonite and associated migmatite constitute a narrow strip that extends for at least 100 km, marking the eastern limit of the Balingup Metamorphic Belt. The monzonite has a Sm–Nd model age of 2.74 ± 0.09 Ga (Fletcher et al., 1983a) and a Rb–Sr model age of c. 2828 Ma (Rosman et al., 1980).

Locality 5: Balingup Metamorphic Belt, granofels

Melanocratic quartz–feldspar–biotite gneiss and granofels outcrops on the southern side of the road (AMG 402800E 6261400N) near Balingup. The gneissic portions have a foliation trending $128/84^\circ\text{S}$, whereas the more granofelsic parts are weakly foliated and characterized by a strong lineation that plunges 34° toward 314° . Lenses of pegmatite lie parallel to the lineation and may have been sweated-out during metamorphism. The granofels consists of a granoblastic aggregate of plagioclase and quartz, with some microcline. Biotite is moderately abundant, strongly aligned, and evenly distributed throughout the rock. Some hornblende is locally present and shows a similar alignment.

Granofelsic rocks of this type are widespread in the Bridgetown–Balingup area of the Balingup Metamorphic Belt. They are interleaved with quartzite, BIF, and layered quartz–feldspar–biotite gneiss, and are interpreted to have been derived from psammopelitic turbiditic material that has been metamorphosed at medium-pressure amphibolite facies.

Days 2 and 3: The Leeuwin Complex

Apart from specific information on the locations to be visited, this excursion guide also presents major- and trace-element geochemical data and nine SHRIMP U–Pb zircon dates obtained on samples from the Leeuwin Complex, together with a discussion of the regional geology. Some of the sampling sites will be visited during the excursion and the implications of these results will be discussed.

Parts of the coastline between Dunsborough and Augusta are incorporated within the Leeuwin–Naturaliste National Park. The region includes many unique natural features, such as spectacular coastline (where the Indian and Southern Oceans meet), limestone caves, Karri forests, and superb local wines. Many of the sites that will be visited are environmentally sensitive and are protected. Rock samples may not be taken from any of the sites in the national park without prior arrangement.

Regional geology

High-grade rocks of the Leeuwin Complex are present between Cape Naturaliste and Cape Leeuwin in the southwestern corner of Western Australia (Fig. 2) and are separated from the Phanerozoic sediments of the Perth Basin to the east by the Dunsborough Fault. The complex consists predominantly of metamorphosed, even-grained and porphyritic alkali granitic rocks, but also includes minor pegmatitic and mafic dykes and disrupted remnants of massive and layered leucogabbro and anorthosite bodies. These rocks have been metamorphosed to upper amphibolite or granulite facies and heterogeneously deformed.

Relatively few detailed investigations have been undertaken on the rocks of the Leeuwin Complex, and its geological history is still poorly known. Wilde and Murphy (1990) subdivided the gneisses of the complex into seven types, largely on the basis of petrographic and mineralogical features (Fig. 2). They interpreted variations in mineral assemblages as showing that metamorphic grades increase northward, from low-pressure amphibolite facies to the south of Margaret River, to low-pressure granulite-facies conditions to the north, with peak metamorphic temperatures of approximately 690°C inferred from two-pyroxene geothermometry. The presence of arfvedsonite in some of the felsic gneisses (i.e. Type 3 gneisses of Wilde and Murphy, 1990) is regarded as diagnostic of 'A-type' granitoid rocks of peralkaline affinity (Loiselle and Wones, 1979), and Wilde and Murphy (1990) proposed that the complex formed within a continental rift environment.

Myers (1994) informally subdivided the gneisses of the Leeuwin Complex into the older Cowaramup gneiss and the younger Hamelin granite. He included the gabbros and anorthosites (referred to as the Augusta Anorthosite Complex) as part of the Cowaramup gneiss. The Hamelin granite was considered to have intruded the Cowaramup gneiss as large sheet-like bodies. Weakly deformed to undeformed pegmatite dykes (containing magnetite, orthopyroxene, garnet, and biotite) and tonalitic dykes were emplaced during or after the peak of granulite-facies metamorphism, and many have been recrystallized in the amphibolite facies during cooling and uplift of the complex.

Extensive Tertiary laterite, sand, and limestone overlie the metamorphic rocks of the Leeuwin Complex. The limestones were formed from wind-blown calcareous sands derived from the west during periods of low sea level. Cave systems have been developed in Recent times by the dissolution of the carbonate within the sands by groundwater flowing along the irregular contact with the impermeable metamorphic basement rocks.

Geochemistry of the Leeuwin Complex

A reconnaissance geochemical and geochronological investigation of the Leeuwin Complex is in progress, in conjunction with detailed mapping undertaken by John Myers (now at the Memorial University of Newfoundland, Canada).

Geochemical data (major and trace elements by x-ray fluorescence, and rare earth elements by inductively coupled plasma mass spectrometry) obtained on samples of felsic gneiss and metamorphosed leucogabbro and anorthosite from the Leeuwin Complex by Nelson (1995) are listed in Table 1. Nine of the samples listed in the table have also been dated by the SHRIMP U–Pb zircon method. Sample localities and the U–Pb zircon dates obtained on these samples are shown in Figure 2. Additional processing of the geochemical data, including that presented by Wilde and Murphy (1990), was undertaken by Wilde (2000) in order to further constrain the evolution of the Leeuwin Complex. Analyses of two samples of leucogabbro are also listed in

Table 1. Geochemical data for selected rocks from the Leeuwin Complex

GSWA no.	112131	112132	112133	112134	112135	112136	112140	112141	112142	112143	112144A	112145
Percentage												
SiO ₂	70.1	70.7	49.2	75.3	72.8	74.1	64.4	71.9	50.3	68.2	73.5	71.3
TiO ₂	0.44	0.40	0.93	0.21	0.27	0.28	0.93	0.39	2.28	0.70	0.20	0.33
Al ₂ O ₃	13.9	14.1	25.6	12.2	14.1	13.1	15.3	12.5	19.1	14.0	13.2	12.0
Fe ₂ O ₃	0.84	1.69	1.67	1.67	0.38	0.34	1.29	2.39	3.06	3.50	0.55	3.98
FeO	3.06	2.16	3.24	0.79	1.76	1.93	3.83	2.09	6.47	2.99	1.66	1.83
MnO	0.07	0.08	0.08	0.06	<0.05	<0.05	<0.05	0.10	0.16	0.09	<0.05	0.11
MgO	0.22	0.18	1.19	<0.05	0.26	0.28	1.20	0.27	2.63	0.49	0.06	0.25
CaO	1.84	1.29	11.50	0.55	1.66	1.60	3.28	1.68	9.83	2.63	1.02	2.01
Na ₂ O	3.41	3.72	3.49	3.72	2.49	2.44	3.45	3.62	4.23	4.35	3.07	4.78
K ₂ O	5.78	6.00	0.85	5.43	6.02	5.49	4.48	4.78	1.33	2.40	6.37	2.69
P ₂ O ₅	0.08	0.05	0.18	<0.05	0.11	0.11	0.25	0.09	0.58	0.13	<0.05	0.06
CO ₂	0.02	0.17	0.29	0.23	0.15	0.20	0.49	0.10	0.02	0.40	0.21	0.02
S	<0.01	<0.01	0.10	<0.01	<0.01	<0.01	<0.01	<0.01	<0.01	0.04	<0.01	<0.01
H ₂ O+	0.29	0.26	0.52	0.18	0.38	0.32	0.65	0.24	0.26	0.40	<0.10	0.34
H ₂ O-	<0.10	<0.10	<0.10	<0.10	<0.10	<0.10	<0.10	<0.10	<0.10	<0.10	<0.10	<0.10
O=S	<0.01	<0.01	0.05	<0.01	<0.01	<0.01	<0.01	<0.01	<0.01	0.02	<0.01	<0.01
Rest %	0.27	0.29	0.21	0.25	0.18	0.17	0.50	0.26	0.22	0.33	0.23	0.34
Total	100.4	101.1	99.0	100.7	100.7	100.4	100.1	100.5	100.5	100.6	100.3	100.1
Parts per million												
Ba	915	452	383	826	627	520	2 152	825	412	982	681	1 025
Cr	<4	<4	10	8	6	<4	11	<4	<4	<4	<4	<4
Cu	<4	<4	5	<4	<4	<4	<4	7	<4	39	<4	<4
Ga	21	23	26	21	17	16	21	18	23	23	22	23
Nb	38	66	13	70	9	12	18	48	21	50	29	69
Ni	5	5	8	5	5	6	8	6	9	4	6	7
Pb	41	29	6	27	53	51	19	22	10	12	44	9
Rb	242	197	17	181	238	241	163	169	27	53	327	40
Sb	<4	<4	<4	<4	<4	<4	<4	<4	<4	<4	<4	<4
Sc	6	2	9	2	4	4	7	7	20	11	<4	6
Sn	5	5	<4	9	<4	<4	<4	7	<4	7	4	9
Sr	108	57	654	40	87	77	262	109	437	186	80	139
Ta	<5	<5	<5	<5	<5	<5	<5	<5	<5	<5	<5	<5
Th	39	41	3	23	36	46	55	17	8	27	44	12
U	3	3	2	2	2	2	<2	2	<2	2	6	<2
V	8	<3	97	4	10	11	69	3	165	9	<3	4
Y	64	98	14	97	51	41	21	78	38	77	77	117
Zn	81	118	48	132	31	38	90	75	100	71	51	55
Zr	438	579	368	374	162	176	655	490	314	808	253	923
La	53.6	185	22.6	120	66.9	72.6	191	92.7	42.3	114	130	117
Ce	133	384	48.6	262	145	159	343	199	91.7	163	253	264
Pr	16.0	44.8	6.30	33.1	16.9	19.1	35.1	24.3	12.0	19.4	28.3	34.4
Nd	58.6	161	24.7	124	60.30	68.9	110	91.3	47.7	68.5	95.9	131
Sm	13.9	29.5	4.90	27.6	13.1	15.3	16.3	20.4	11.1	15.9	20.4	30.7
Eu	2.98	2.67	2.41	4.43	1.94	1.65	3.37	3.89	3.56	1.83	2.85	6.95
Gd	15.4	36.0	5.50	32.6	14.9	17.6	19.0	24.2	12.8	18.0	24.2	35.8
Tb	2.30	4.30	0.60	4.40	1.80	2.20	1.30	3.18	1.70	2.20	3.20	5.10
Dy	11.70	20.50	2.60	23.10	9.60	9.50	4.00	17.30	8.70	9.70	16.60	26.5
Ho	2.40	3.90	0.50	4.70	2.10	1.70	0.70	3.60	1.70	1.80	3.10	5.40
Er	6.90	11.30	1.60	12.70	7.10	5.00	1.90	9.80	4.70	5.10	9.40	15.1
Tm	1.00	1.50	0.20	1.80	1.10	0.70	0.20	1.60	0.70	0.70	1.40	2.20
Yb	6.40	9.30	1.50	11.4	7.0	4.20	0.90	9.50	4.20	4.20	8.30	12.9
Lu	0.90	1.50	0.20	1.60	1.0	0.60	0.10	1.40	0.60	0.60	1.20	1.90

NOTES: 112131: Coarse, porphyritic (augen) granite gneiss, Cape Leeuwin, south of lighthouse (AMG 328600E 6194400N)
 112132: Even-grained granite gneiss, Sarge Bay (AMG 328600E 6195300N)
 112133: Anorthosite, Cape Leeuwin road near Skippy Rock road turn-off (AMG 331200E 6197300N)
 112134: Fine-grained granite, Cosy Corner (AMG 318200E 6207800N)
 112135: Augen gneiss, Redgate Beach – Isaacs Rock, north of monument (AMG 315300E 6231077N)
 112136: Augen gneiss, Redgate Beach – Isaacs Rock (AMG 315200E 6231600N)
 112140: Grey, fine-grained granite dyke, from coastal exposure south of Gracetown (AMG 313200E 6249600N)
 112141: Coarse, even-grained granite gneiss, from coastal exposure south of Gracetown (AMG 313200E 6249600N)
 112142: Leucogabbro, coast north of Cowaramup Bay (AMG 313800E 6252200N)
 112143: Medium-grained granite gneiss, coast north of Cowaramup Bay, sampling site is 20 m north of 112142 (AMG 313800E 6252200N)
 112144A: Coarse, porphyritic (augen) granite gneiss, headland south of Smith's Beach, Canal Rocks North (AMG 315500E 6273700N)
 112145: Fine, even-grained, pink, granulite-facies granite, west of Meelup Beach at Gannet Rock (AMG 322400E 6283900N)

Table 1: the Cape Leeuwin anorthosite (112133) at excursion Locality 7, and a leucogabbro (112142) from a coastal exposure north of Cowaramup Bay, at excursion Locality 13.

Wilde and Murphy (1990) argued that the depletion in large-ion lithophile elements shown by many granulites is absent in the Leeuwin Complex gneisses. The results obtained by Nelson (1995) confirm this finding. The precursors to the felsic gneisses are mainly alkali granites characterized by relatively high K_2O , Na_2O and generally high K_2O/Na_2O . In terms of alkalinity index (Fig. 4), the rocks from both datasets show a spread from peraluminous to metaluminous, with only one rock (Type 4 gneiss sample 12202 from approximately 12 km south of Cape Naturaliste) being peralkaline. Although a Sr–CaO plot reveals a distinct positive correlation, and there are well-defined negative correlations between $CaO-SiO_2$, total $Fe-SiO_2$, and TiO_2-SiO_2 (Wilde, 2000) that suggest that the rocks evolved by a common magmatic process, this is difficult to substantiate in view of the range in ages revealed by the rocks, as discussed below.

Rare-earth element (REE) plots for the rocks listed in Wilde and Murphy (1990) are presented in Figure 5 a to d (Wilde, 2000) and those of Nelson (1995) are shown in Figure 6. The Wilde and Murphy (1990) data support the distinction between gneiss types recognized from field, modal, and major-element geochemical characteristics, with a range in light rare-earth element enrichment and the intensity of the negative Eu anomaly. Although there is no distinct trend indicative of simple fractionation, there is a range to slightly higher La values in some samples, with La/Sm ratios of between 4 and 7 (Wilde, 2000). The alkali granites analysed by Nelson (1995) display generally parallel patterns, with slight enrichment in the light rare-earth elements relative to the heavy rare-earth elements, and with pronounced negative Eu anomalies (Fig. 6). These

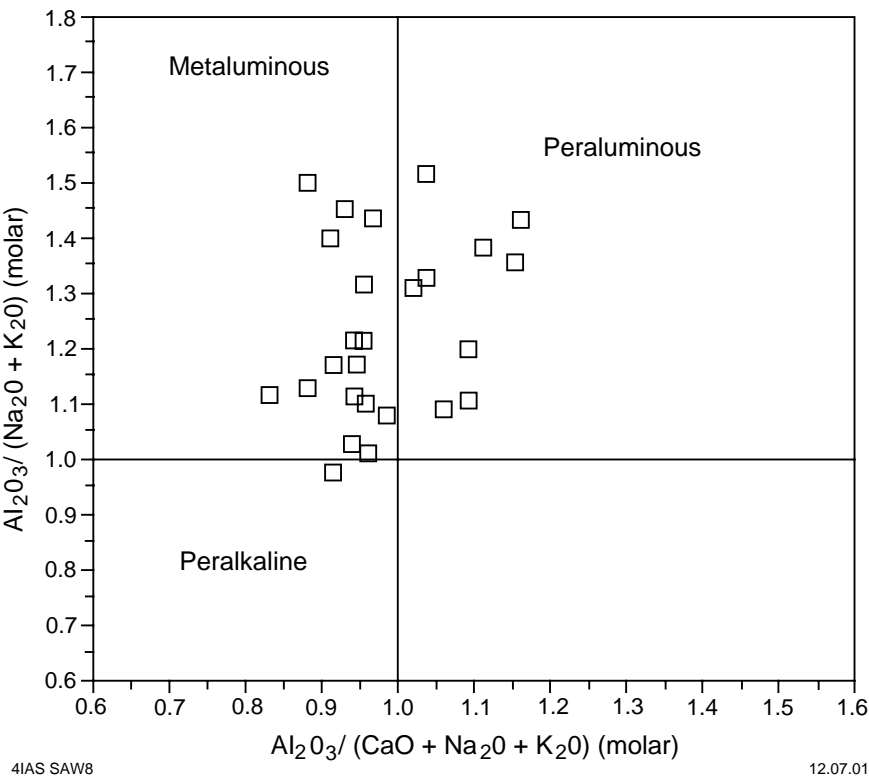


Figure 4. Shand $Al_2O_3/(Na_2O+K_2O) - Al_2O_3/(CaO+Na_2O+K_2O)$ (molecular values) diagram showing alkalinity index of the Leeuwin granitoids analysed by Wilde and Murphy (1990) and Nelson (1995)

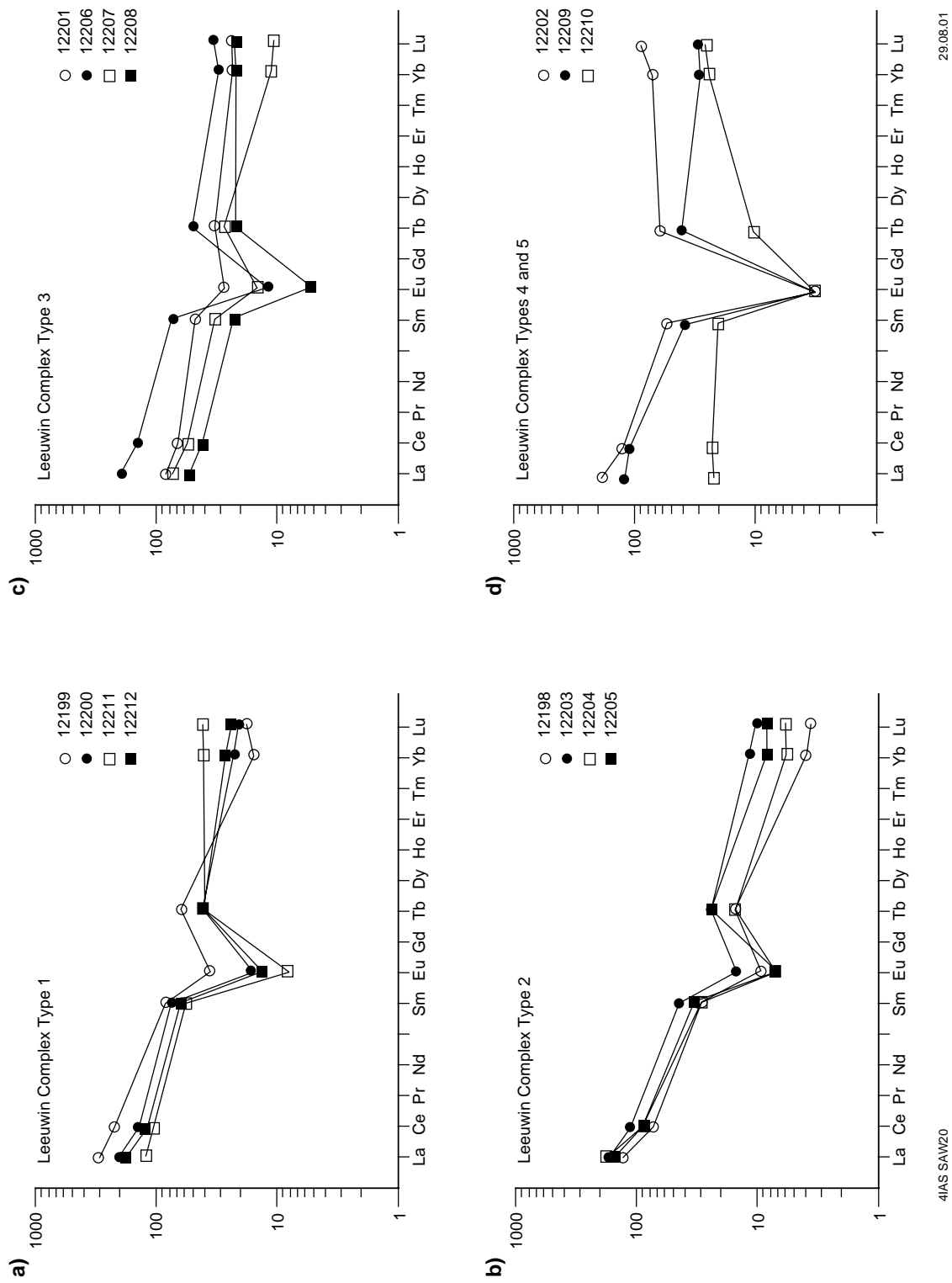


Figure 5. Chondrite-normalized rare earth-element diagrams for granitoid rocks from the Leeuwin Complex analysed by Wilde and Murphy (1990). Gneiss types as classified in Figure 2: (a) Type 1 gneisses, (b) Type 2 gneisses, (c) Type 3 gneisses, (d) Type 4 and 5 gneisses. Numbers refer to samples listed in Wilde and Murphy (1990). Modified from Wilde (2000)

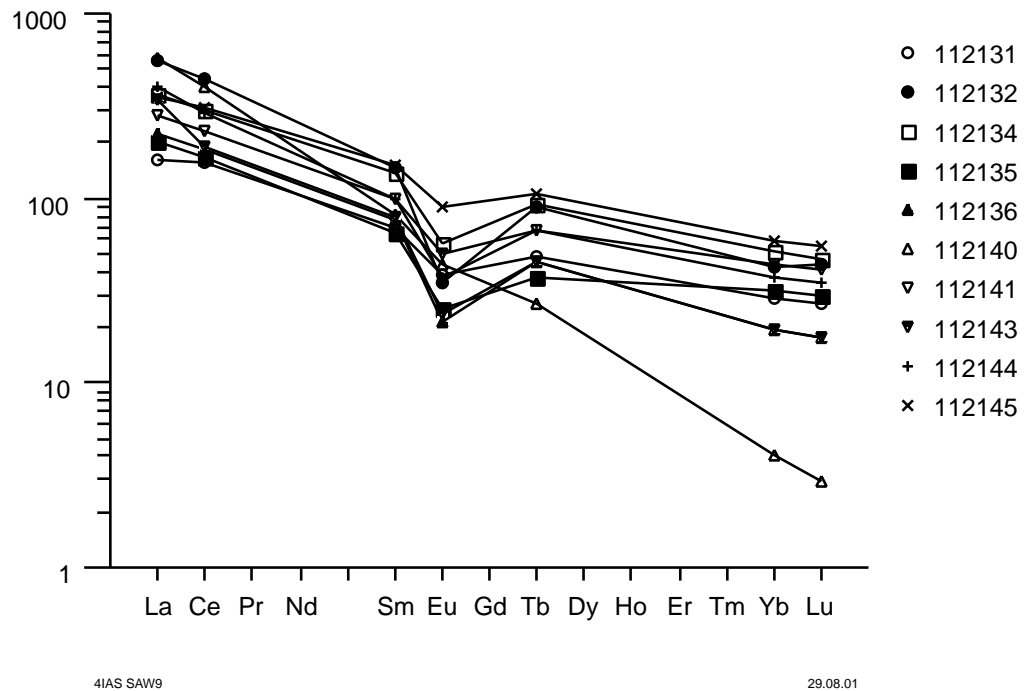


Figure 6. Chondrite-normalized rare-earth element plot for samples from the Leeuwin Complex (modified from Nelson, 1995)

patterns are typical of granitoid magmas derived from intracrustal sources where plagioclase is stable within the source. The similarity in the rare-earth element profiles (with the notable exception of 112140, the granite dyke from south of Gracetown) is again consistent with the hypothesis that the alkali granites were derived from a common crustal source.

The rare-earth element patterns for the Cape Leeuwin anorthosite (112133) and the Cowaramup Bay leucogabbro (112142) are parallel to those of the alkali granites (Fig. 6), but at considerably lower overall rare-earth element abundances. The pattern of the Cowaramup Bay leucogabbro lacks a significant Eu anomaly and the Cape Leeuwin anorthosite pattern shows a positive Eu anomaly, consistent with an origin for the anorthosite from a differentiated mafic intrusion. These geochemical data indicate that the rare-earth element patterns of the alkali granites could have been produced by the partial melting of lower crustal sources having rare-earth element characteristics similar to those of the Cape Leeuwin anorthosite (112133) and the Cowaramup Bay leucogabbro (112142). The rare-earth element pattern of the Cowaramup Bay granite dyke (112140) is considerably steeper than those of the other granites, indicating that the granite dyke was derived from a chemically or mineralogically different source — possibly from a deeper, garnet-bearing source.

A positive correlation between CaO (wt%) and Eu/Eu^* for samples from the Leeuwin Complex, with the anorthosite and leucogabbro samples plotting along an extension of the trend displayed by the alkali granite samples, demonstrates that the degree of the Eu depletion is strongly correlated with the CaO content of the samples. The negative Eu anomalies of the alkali granites are most probably due to retention of Eu within plagioclase-rich sources rather than high-level crystal fractionation processes.

¹ Eu/Eu^* denotes the ratio of the measured Eu abundance to the theoretical abundance (Eu^*), calculated assuming a smooth chondrite-normalized rare-earth element pattern in the region Sm–Eu–Gd.

When plotted on the Rb-(Yb+Ta) discriminant diagram of Pearce et al. (1984), the rocks largely fall in the 'within plate granite' field (Wilde, 2000). Similarly, on the cationic plot of Batchelor and Bowden (1985; Fig. 7), the rocks show a strong linear grouping mostly falling in the 'anorogenic' field, with only slight overlap into the 'late-orogenic' and 'post-orogenic' fields, thus supporting the original view of Wilde and Murphy (1990) that the rocks were derived from melting of pre-existing crust.

SHRIMP U–Pb zircon data (see below) indicate that the igneous precursors to the felsic gneisses of the Leeuwin Complex crystallized over a period of at least 500 million years and therefore could not have been derived from a common parental alkali granite magma. Sm–Nd isotopic analyses of felsic gneiss samples from the Leeuwin Complex (McCulloch, 1987; Black et al., 1992; Fletcher and Libby, 1993), in combination with the new geochronological data obtained in this study, indicate that the precursors to the felsic gneisses were emplaced with highly negative ϵ_{Nd} values, and suggest that they were derived by the melting of crustal sources that included components formed during or prior to the Mesoproterozoic.

The ages of the leucogabbro and anorthosite components of the Leeuwin Complex are uncertain. Black et al. (1992) stated that McCulloch (unpublished data) obtained a SHRIMP U–Pb zircon date of about 700 Ma for a hornblende meta-anorthosite. However, in this study, insufficient zircon was recovered from a sample of anorthosite (112133) taken from a site inferred to be near that of McCulloch. It is possible that the zircons isolated by McCulloch from the hornblende meta-anorthosite sample may have been derived from the c. 685 Ma alkali granite precursors to the gneisses that vein the

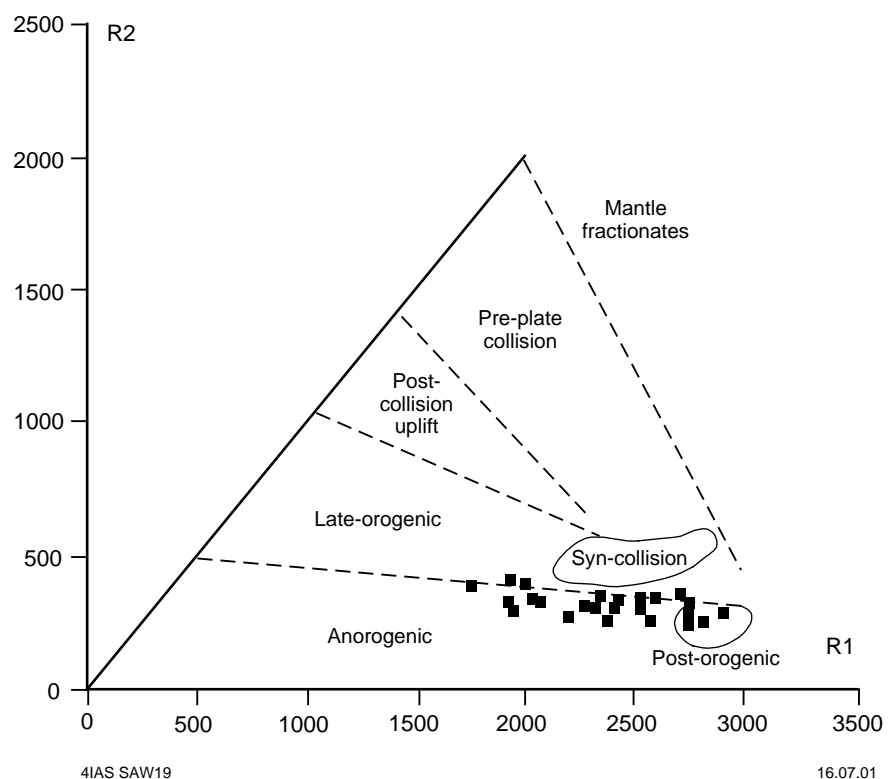


Figure 7. The de la Roche diagram of Batchelor and Bowden (1985) indicating that the Leeuwin Complex samples of Wilde and Murphy (1990) and Nelson (1995) plot mainly in the 'anorogenic' field. The data are calculated as cations, with $R1 = 4\text{Si} - 11(\text{Na} + \text{K}) - 2(\text{Fe} + \text{Ti})$ and $R2 = 6\text{Ca} + 2\text{Mg} + \text{Al}$ (modified from Wilde, 2000)

anorthosites in the southern part of the Leeuwin Complex. The leucogabbro and anorthosite components were affected by the c. 615 Ma metamorphic event and, on the basis of field observations near Cape Leeuwin, are older than the c. 685 Ma alkali granite precursors to the gneisses in this area.

Other Proterozoic occurrences of leucogabbroic and anorthositic rocks are commonly associated with alkali granitic intrusions. Examples include the Laramie Anorthosite Complex associated with K₂O-rich granitoid rocks of the Sherman batholith (Frost et al., 1994), the massif anorthosites of the Adirondack Mountains that occur with syenitic granites (McLelland et al., 1994), and the Chilka Lake Anorthosite complex of the Eastern Ghats of India, argued by Sarkar et al. (1981) to be genetically related to closely associated alkali granites.

Previous geochronology

Compston and Arriens (1968) obtained a combined Rb–Sr isochron age of 655 ± 25 Ma on whole-rock and mineral samples of gneiss and pegmatite collected near Sugarloaf Rock. This was interpreted as the time of regional granulite-facies metamorphism. Fletcher et al. (1985) and Fletcher and Libby (1993) reported Sm–Nd depleted-mantle model ages of 2060–2010 Ma for gneisses recovered from boreholes penetrating the Perth Basin to the east of the Leeuwin Complex. These gneisses are part of the Darling Mobile Belt, but are not from the Leeuwin Complex. McCulloch (1987) and Fletcher and Libby (1993) obtained substantially younger Sm–Nd depleted-mantle model ages of 1180 to 1135 Ma on gneisses from near Sugarloaf Rock and Sarge Bay. Wilde and Murphy (1990) reported a conventional U–Pb zircon date of 570 to 550 Ma from a granitic gneiss taken from a site near Meelup, northwest of Dunsborough. This was interpreted as dating igneous emplacement of the granitic precursor to the gneiss. A further two Sm–Nd model ages of 1290 and 1560 Ma were listed by Black et al. (1992) for Leeuwin Complex granitic gneisses from undisclosed localities. Black et al. (1992) also revealed that McCulloch (unpublished data) obtained SHRIMP U–Pb zircon dates of about 700 and 500 Ma for hornblende anorthosite and leucogranite samples, respectively, from the Leeuwin Complex, but no further details about the samples or the results obtained were given.

Geochronological data are discussed below, with reference to excursion localities.

Geological evolution of the Leeuwin Complex

The geological history of the Leeuwin Complex is summarized in Table 2. The field, petrographic, and geochronological data presented here indicate that peak metamorphic conditions occurred at c. 615 Ma, that the complex experienced upper amphibolite-facies metamorphism following emplacement of the 540 ± 6 Ma alkali granite precursor to the Cowaramup Bay hornblende–biotite monzogranite gneiss (112143), and that the metamorphic grade was low during intrusion of the 524 ± 12 Ma Gracetown biotite–hornblende monzogranite dyke.

The geochronology data summarized in this excursion guide can contribute to discussion about the origin of the Leeuwin Complex in the context of the late Proterozoic to early Phanerozoic development of Gondwanaland. Reconstruction of the relative positions of the Gondwanaland continents in the early Phanerozoic (Oliver et al., 1983) generally place the southwestern corner of Western Australia adjacent to the Bungar Hills region near the coast of east Antarctica. A conventional U–Pb zircon date of 516 ± 1.5 Ma was obtained by Black et al. (1992) for a syenite from David Island, in the Denman Glacier region to the west of the Bungar Hills. Black et al. (1992) also obtained a SHRIMP U–Pb zircon lower concordia intercept date of 567 ± 49 Ma,

Table 2. Summary of the geological history of the Leeuwin Complex

<i>U–Pb zircon age (Ma)</i>	<i>Interpretation</i>
525	Intrusion of syenite and granite dykes at low metamorphic grade
540	Emplacement of alkali granite; deformation and recrystallization within the amphibolite facies during slow uplift and cooling
c. 615	Metamorphism in the granulite facies
705–680	Emplacement of alkali granite
c. 680	Emplacement and differentiation of mafic intrusions within the lower crust (or ponding and differentiation of mafic magma at the crust–mantle boundary)
780	Emplacement of alkali granite
1090	Emplacement of alkali granite
1180	Xenocryst zircons possibly derived from the source regions of 1090 Ma alkali granite precursors to the gneisses at Isaacs Rock/Redgate Beach

interpreted as the time of high-grade metamorphism, from a tonalitic orthogneiss from Cape Charcot, further to the west of the Denman Glacier. Based on garnet–whole-rock Sm–Nd dating, Hensen and Zhou (1995) argued that gneisses from the Prydz Bay region of east Antarctica, about 750 km to the west of the Denman Glacier, had also experienced a granulite-facies metamorphic event at c. 500 Ma. Furthermore, the Lützow–Holm and Yamato–Belgica Complexes, located more than 2400 km to the west of the Denman Glacier on the Prince Olav Coast, also record a high-grade regional metamorphism and deformation event between 555 and 520 Ma (Shiraishi et al., 1994). These studies indicate that late Proterozoic to early Phanerozoic (or Pan-African) metamorphism may have affected a large region of east Antarctica. Significantly, throughout east Antarctica, this metamorphic episode is generally a high-temperature, low-pressure event (Tingey, 1991; Hensen and Zhou, 1995), as in the Leeuwin Complex. These results indicate that high-grade metamorphism in the Leeuwin Complex and in parts of east Antarctica were roughly synchronous and that these areas share at least part of a common geological history.

Most continent reconstructions of Gondwanaland place northern India adjacent to the present west coast of Western Australia during the early Phanerozoic, so it is instructive to compare the geological evolution of the Leeuwin Complex with that of India. Within the Southern Granulite domain of peninsular India, alkali granites and syenites were emplaced between 750 and 500 Ma, and charnockites have been dated at 564 to 540 Ma (Unnikrishnan-Warrier et al., 1993). Anorthosite complexes occur in association with alkaline intrusions in the Eastern Ghats region of India. One of these, the Chilka Lake Anorthosite, has been dated by the whole-rock Rb–Sr method at c. 1400 Ma (Sarkar et al., 1981). A high-grade metamorphic event between 610 and 550 Ma has also been documented for Sri Lanka (Shiraishi et al., 1994). Although there is considerable debate about the relative positions of India, Sri Lanka, and Antarctica during the early Phanerozoic, it is likely that parts of southern and eastern India, Sri Lanka, east Antarctica, and the Leeuwin Complex of Western Australia were closely associated at this time (Fig. 3).

It is generally thought that A-type granites can be formed in both post-orogenic and anorogenic settings (Whalen et al., 1987, 1996; Sylvester, 1989; Bonin, 1990; Eby, 1992), and that the post-orogenic A-type granites differ in having higher magmatic

temperatures and more primitive isotopic signatures. The A-type granitic magmatism and subsequent metamorphism of the Leeuwin Complex has been linked by Wilde (2000) to reworking of the Darling Mobile Belt. Alternatively, as with parts of the Albany–Fraser Orogen (Nelson et al., 1995), it is possible that the Leeuwin Complex is an exotic continental fragment that once formed part of present-day east Antarctica, and that it has been tectonically transported (possibly by early strike-slip movement along the Darling Fault) to its present position in Western Australia during the early break-up of the Gondwanaland continents and the movement of India northwards relative to Australia and Antarctica. Further work is required in order to differentiate between these hypotheses.

Locality 6: Pegmatite-banded granite gneiss, leucogabbro, and amphibolite, Skippy Rock

Pegmatite-banded granitic gneisses, leucogabbros, and amphibolites are exposed in the rock pavement immediately west of the car park at Skippy Rock (AMG 327700E 6196700N). Two main igneous associations are present: a fine-, even-grained, biotite–hornblende orthogneiss with abundant pegmatite dykes, and a fine-, even-grained leucogabbro containing irregular zones and lenses of amphibolite, and net-veined by very coarse grained plagioclase–hornblende dykes. Both associations have been strongly deformed and recrystallized. Granitic dykes are not present within the leucogabbro, and the very coarse grained plagioclase–hornblende dykes have not intruded the granitic gneiss. The two associations may have been brought into tectonic contact by the deformation episode during which the steeply dipping, north–south-trending foliation developed.

According to Myers (1990, 1994), the anorthosite is in a belt about 1.5 km wide that may represent a large isoclinal fold with an undulating subhorizontal plunge.

Locality 7: Anorthosite, Cape Leeuwin – Skippy Rock roads

At this locality (Cape Leeuwin road south of the Skippy Rock road turn-off; AMG 331200E 6197300N), a coarse-grained anorthosite containing labradorite (An_{62}), olive-green hornblende and minor opaques, titanite, accessory apatite, chlorite, biotite, prehnite, microcline, muscovite, and calcite can be seen. Deformation is heterogeneous and the rock has been thoroughly recrystallized under medium- to high-grade conditions, although igneous textures are still preserved. Large (up to 50 mm in diameter) deformed relict orthopyroxene oikocrysts are present, and irregular, diffuse pegmatitic melt patches and veins are common. Some of the pegmatitic melt patches crosscut the foliation and are undeformed.

Geochemical data obtained on a sample taken near this site (112133, taken from the eastern side of the Cape Leeuwin road and 50 m north of the Skippy Rock road turn-off) are given in Table 1. This sample did not contain sufficient zircon for analysis.

Locality 8: Hornblende granite gneiss, Sarge Bay

An even-grained granite gneiss is present at this locality (AMG 328600E 6195300N). A sample (GSWA 112132) was taken at Sarge Bay, north of the Cape Leeuwin road leading to Cape Leeuwin lighthouse and immediately east of the junction with the Skippy Rock road. A geochemical analysis is given in Table 1. The sample is a medium-grained (approximately 1 mm) granoblastic gneiss consisting of perthitic microcline, quartz, and plagioclase, with lesser hornblende (dark-green hastingsite with low 2V), minor biotite and accessory opaques, titanite, apatite, and zircon. Distinctive features

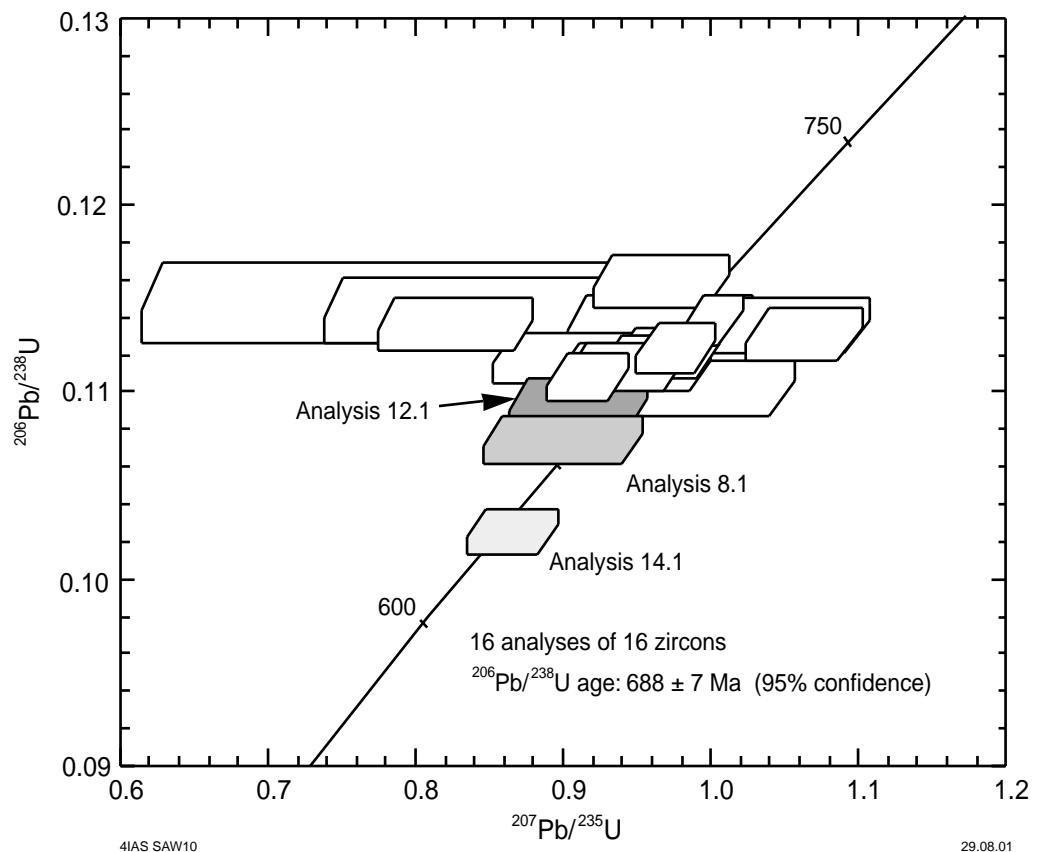


Figure 8. Concordia diagram for 112132: granite gneiss, Cape Leeuwin lighthouse road

are the relatively low quartz content for a granite and the abundant accessory zircon and titanite. The original rock was an iron-rich granite metamorphosed to amphibolite or lower granulite facies.

Most of the zircons extracted from this sample were clear to pale yellow, subhedral to anhedral, averaged $200 \times 75 \mu\text{m}$ in size, and lacked obvious internal structure. Many had mineral and fluid inclusions. Nineteen analyses were obtained on 19 zircons. Results are shown on a concordia plot in Figure 8. Sixteen analyses have $^{206}\text{Pb}/^{238}\text{U}$ ratios almost within error of a single value (chi-squared = 1.11) and indicating an age of $688 \pm 7 \text{ Ma}$. This is interpreted as the time of igneous crystallization of the granite precursor to the gneiss. Three analyses (12.1, 8.1, and 14.1) have $^{207}\text{Pb}/^{206}\text{Pb}$ ratios indistinguishable from the main population, but have slightly lower $^{206}\text{Pb}/^{238}\text{U}$ ratios. These analyses have probably been disturbed during the metamorphic event following crystallization of the granite precursor to the gneiss.

Locality 9: Hornblende granite gneiss, Cape Leeuwin

The rock platform south of the Cape Leeuwin lighthouse (AMG 328600E 6194400N) consists of coarse porphyroclastic (augen) granite gneiss. The gneiss has coarse pegmatites generally about 30 cm thick that have intruded parallel to a steeply dipping north–south foliation (350° /subvertical) and that are boudinaged, thus causing deflection of the earlier foliation. Some pegmatites post-date the deformation. A geochemical analysis of a sample of this gneiss (112131) is given in Table 1. The gneiss consists of a medium-grained (approximately 2 mm), moderately foliated granoblastic assemblage

of perthitic microcline, quartz, and oligoclase, with lesser amounts of hornblende and biotite, and accessory opaques, apatite, and zircon. Minor garnet is also present. Microcline crystals are up to 6 mm across and enclose small quartz and plagioclase grains. Plagioclase crystals are commonly up to 2 mm across. Many feldspar grains are separated by a narrow zone of clear albite or untwinned K-feldspar. Hornblende is a dark-green hastingsitic variety with low 2V, and forms trains that outline the foliation in the rock. Biotite forms thin plates up to 3 mm long, and commonly shows dark oxidized margins. The original rock was an iron-rich granite, metamorphosed to medium grade or lowest high grade.

Most of the zircons extracted from this sample were clear to pale yellow, subhedral to anhedral or metamorphically rounded and corroded, averaged $200 \times 75 \mu\text{m}$ in size, and lacked obvious internal structure. Many had mineral and fluid inclusions. Sixteen analyses were obtained on 16 zircons. Results are shown on a concordia plot in Figure 9. All 16 analyses have $^{206}\text{Pb}/^{238}\text{U}$ ratios almost within error of a single value (chi-squared = 1.49) and indicating an age of $681 \pm 10 \text{ Ma}$. This is interpreted as the time of igneous crystallization of the granite precursor to the gneiss.

Locality 10: Granite gneiss, Cosy Corner

A light pink-orange, even-grained granitic gneiss is present at Cosy Corner (AMG 318200E 6207800N). The gneiss is derived from a medium-grained granitoid and is weakly foliated and granoblastic. Principal minerals are perthite, quartz, and albite, with minor opaque oxides and altered amphibole, and accessory titanite, zircon, calcite, and chlorite. Much of the perthite has unmixing to microcline with veins of albite, and to discrete grains of microcline and poorly twinned albite. A few grains of original plagioclase are probably oligoclase in composition. Original amphibole has been altered to secondary iron oxides fringed by arfvedsonite. Titanite forms rounded blebs throughout the rock. The gneiss contains nebulous coarse-grained, irregular pegmatitic

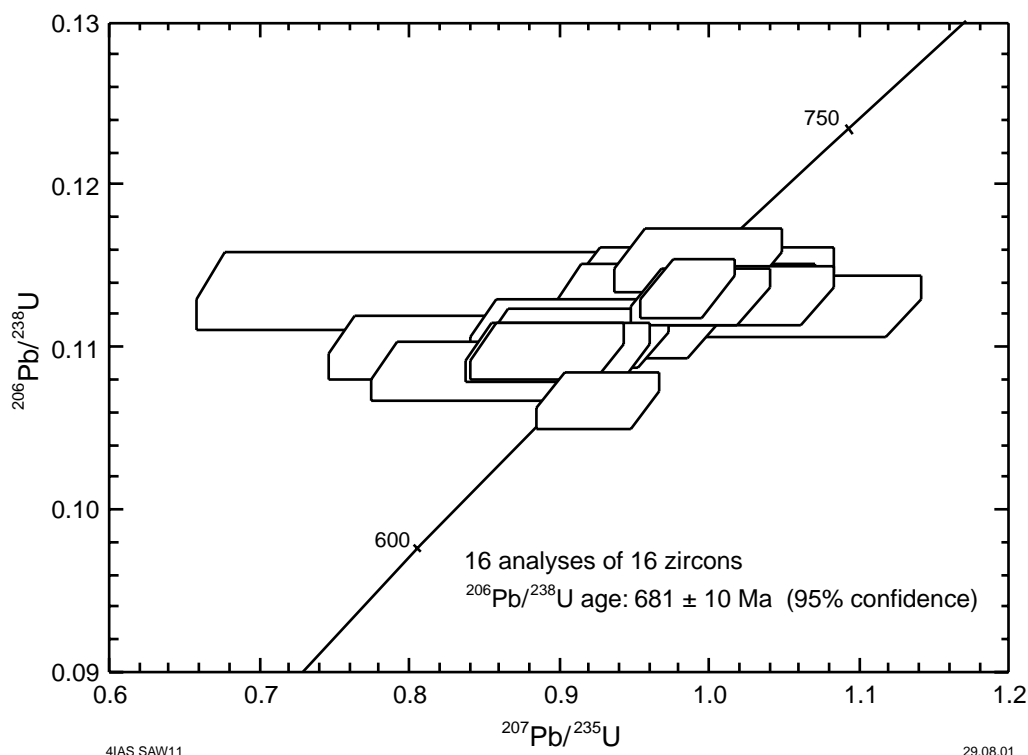


Figure 9. Concordia diagram for 112131: granite gneiss, Cape Leeuwin lighthouse

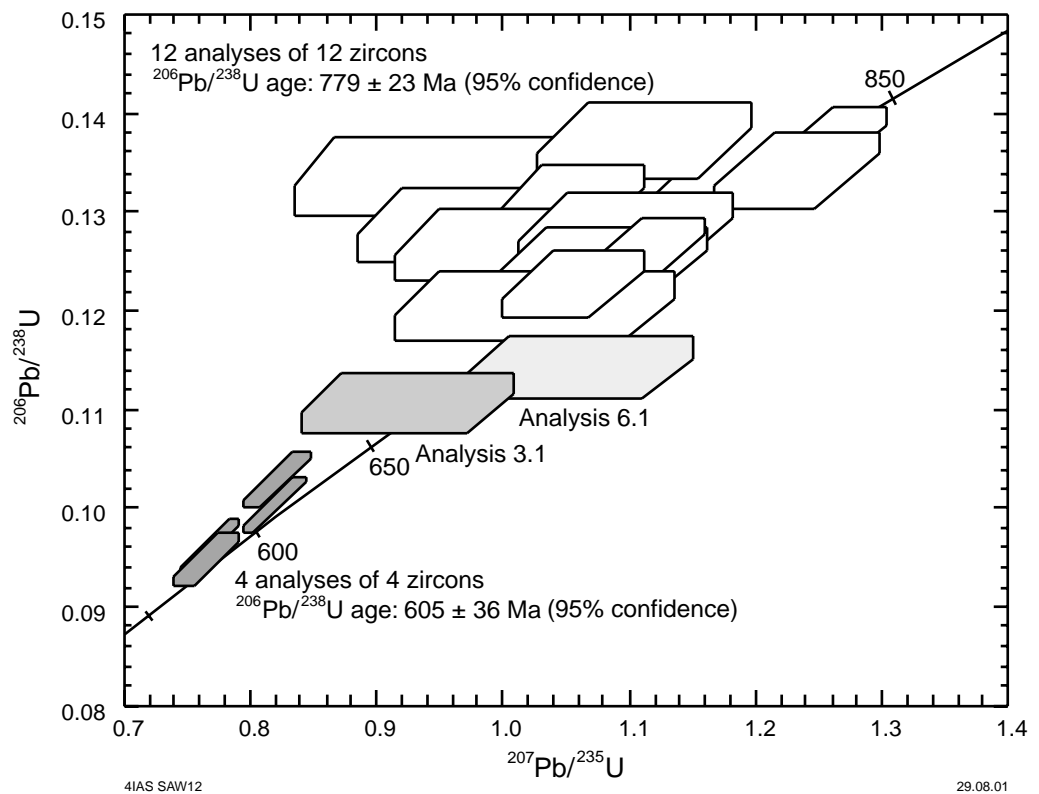


Figure 10. Concordia diagram for 112134: granite gneiss, Cosy Corner

patches and veins, and has also been intruded by coarse pegmatite dykes that post-date the main phase of deformation. GSWA sample 112134 was taken from among the boulders to the west of the car park. A geochemical analysis of this sample is given in Table 1.

Most of the zircons extracted were clear to pale yellow, subhedral to anhedral, averaged $350 \times 100 \mu\text{m}$ in size, and lacked obvious internal structure. Eighteen analyses were obtained on 18 zircons. Results are shown on a concordia plot in Figure 10. All analyses can be placed into four groups. Group 1, consisting of 12 analyses, has $^{206}\text{Pb}/^{238}\text{U}$ ratios almost within error of a single value (chi-squared = 1.98) and indicating an age of $779 \pm 23 \text{ Ma}$. This is interpreted as the time of igneous crystallization of the granite precursor to the gneiss. Groups 2 and 3, consisting of one analysis each (analyses 3.1 and 6.1 respectively), have slightly lower $^{206}\text{Pb}/^{238}\text{U}$ ratios and are probably disturbed members of Group 1 or are of sites that include both Group 1 and 4 components. Group 4 consists of four analyses of zircons morphologically similar to those of the other groups, but having substantially higher U concentrations (650–1327 ppm) and lower Th/U ratios. These have $^{206}\text{Pb}/^{238}\text{U}$ ratios almost within error of a single value (chi-squared = 1.45) and indicating an age of $605 \pm 36 \text{ Ma}$. These zircons were probably derived from the nebulous melt patches. If this interpretation is correct, Group 4 analyses probably indicate the time of peak metamorphic conditions.

Locality 11: Garnet–biotite–quartz–feldspar augen gneiss, Isaacs Rock

Strongly foliated, medium-grained biotite augen gneiss is present west of the car park at Isaacs Rock, north of Redgate Beach. The gneiss contains coarse, light pink-orange,

irregular pegmatitic patches as stringers and lenses elongated parallel to a horizontal foliation. Rare pegmatite dykes were emplaced late during, or following, the deformation. All phases have been recrystallized, and patches with dark-red garnets approximately 4 mm in size are present.

Two samples have been dated from this site. Sample 112135, a garnet–biotite–quartz–feldspar augen gneiss, was sampled north of the monument at Isaacs Rock (AMG 315300E 6231700N). This sample consists of a medium- to coarse-grained, granoblastic assemblage of quartz, calcic oligoclase, and microcline, with lesser biotite and scattered porphyroblasts of garnet. Accessory minerals include zircon, apatite, and opaque oxides. The general texture is an oriented polygonal mosaic, with grain size of 0.5 to 1.5 mm and irregular porphyroblasts of garnet up to 3 mm across. The original rock was probably a monzogranite that was metamorphosed at medium to high grade.

The zircons extracted from this sample are commonly colourless to pale green-yellow, elongate, subhedral with rounded terminations, and between $40 \times 100 \mu\text{m}$ and $80 \times 350 \mu\text{m}$ in size. Many grains are structureless, although grains displaying strong internal zonation are also common. A minority of grains have small rounded cores. Twenty-four analyses were obtained from 24 zircons. Results are shown on a concordia plot in Figure 11. Most analyses are concordant or show slightly normal and reverse discordance, with the discordance pattern consistent with the recent redistribution of radiogenic Pb within the analysis sites. Eighteen analyses of 18 zircons have $^{207}\text{Pb}/^{206}\text{Pb}$ ratios defining a single population and indicating a weighted mean date of $1091 \pm 8 \text{ Ma}$ (chi-squared = 0.99). Analyses 2.1, 3.1, and 4.1 have $^{207}\text{Pb}/^{206}\text{Pb}$ ratios defining a single population and indicating a weighted mean date of $1178 \pm 40 \text{ Ma}$ (chi-squared = 0.26). Analyses 5.1 and 6.1 indicate a weighted mean date of $1016 \pm 10 \text{ Ma}$.

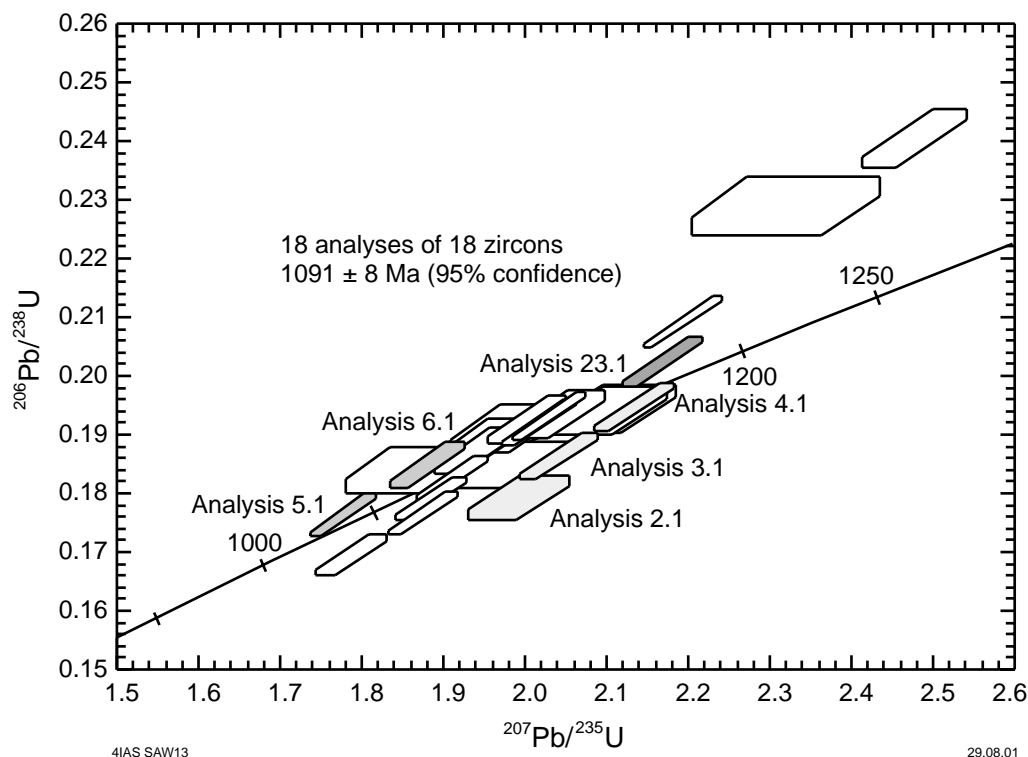


Figure 11. Concordia diagram for 112135: augen gneiss, Redgate Beach

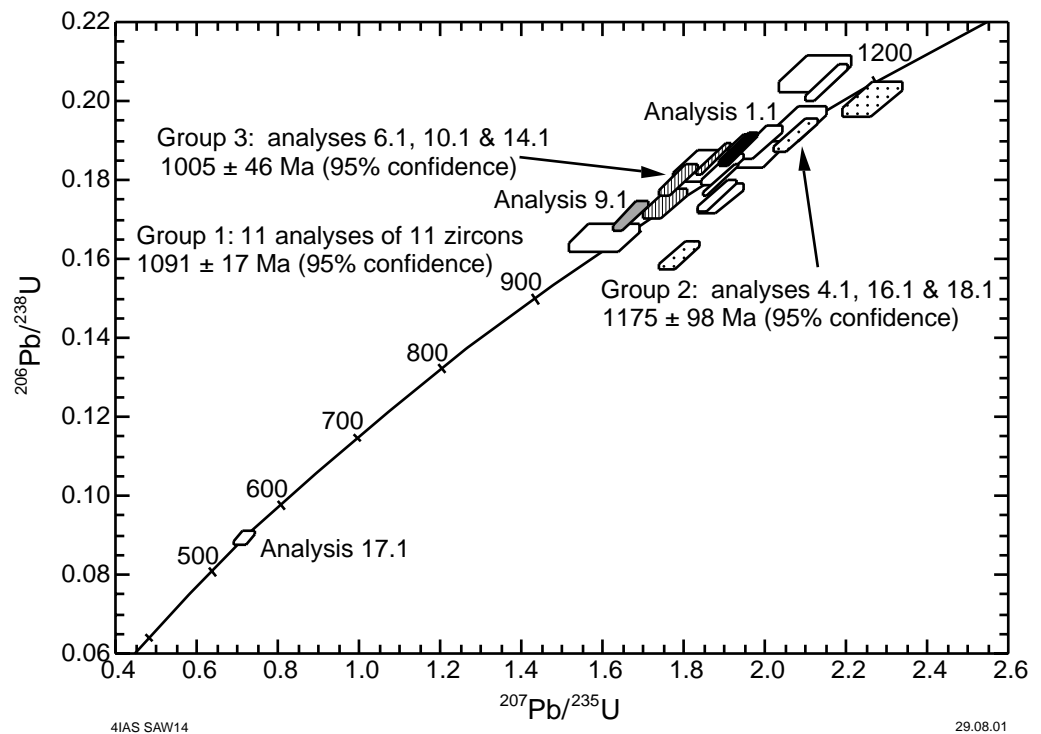


Figure 12. Concordia diagram for 112136: augen gneiss, Redgate Beach

The date of 1091 ± 8 Ma indicated by the 18 analyses of 18 zircons is interpreted as the time of igneous crystallization of the monzogranitic precursor to the gneiss. Analyses 2.1, 3.1, 4.1, and analysis 23.1 are interpreted to be of xenocryst zircons from the source region. Analyses 5.1 and 6.1, obtained from sites having generally high uranium contents, are interpreted to be of sites that have lost some radiogenic Pb.

Sample 112136 was taken from near the monument at Isaacs Rock, to the south of the sampling site of 112135 (AMG 315300E 6231600N). This garnet–biotite–quartz–feldspar augen gneiss consists of a coarse-grained granoblastic assemblage of quartz, calcic oligoclase, and microcline grains up to 6 mm across, with lesser biotite and scattered porphyroblasts of garnet. Accessory minerals include zircon, apatite, and opaque oxides. Secondary calcite and chlorite are present. The general texture is an oriented polygonal mosaic, with grain size of 0.5 to 1.5 mm. The original rock was probably a porphyritic monzogranite metamorphosed at medium to high grade.

The zircons extracted from this sample are commonly colourless to pale green-yellow, elongate, subhedral with rounded terminations, and between $40 \times 100 \mu\text{m}$ and $12 \times 450 \mu\text{m}$ in size. Many grains are structureless, although grains displaying strong internal zonation are also common. A minority of grains have small rounded cores. Twenty analyses were obtained from 20 zircons. Results are shown on a concordia plot in Figure 12. Most analyses are concordant or show slightly normal and reverse discordance, with the discordance pattern consistent with recent redistribution of radiogenic Pb within the analysis sites. Many analyses may be assigned to three groups on the basis of their $^{207}\text{Pb}/^{206}\text{Pb}$ ratios. Eleven analyses of 11 zircons, assigned to Group 1, have $^{207}\text{Pb}/^{206}\text{Pb}$ ratios defining a single population and indicating a weighted mean date of 1091 ± 17 Ma (chi-squared = 1.37). Analyses 4.1, 16.1 and 18.1, assigned to Group 2, have $^{207}\text{Pb}/^{206}\text{Pb}$ ratios defining a single population and indicating a weighted mean date of 1175 ± 98 Ma (chi-squared = 1.44). Analyses 6.1, 10.1 and 14.1, assigned

to Group 3, have $^{207}\text{Pb}/^{206}\text{Pb}$ ratios defining a single population and indicating a weighted mean date of 1005 ± 46 Ma (chi-squared = 0.82). Analyses 1.1 and 9.1 cannot be assigned to any of these three groups. Concordant analysis 17.1, obtained on a clear, structureless rim, has a substantially younger $^{207}\text{Pb}/^{206}\text{Pb}$ date.

The date of 1091 ± 17 Ma indicated by the 11 analyses of 11 zircons of Group 1 is interpreted as the time of igneous crystallization of the porphyritic monzogranitic precursor to the gneiss. This date is within error of the date of 1091 ± 8 Ma obtained for the time of igneous crystallization of sample 112135, taken from a site nearby. The date of 1175 ± 98 Ma indicated by the analyses of Group 2 is within error of the date of 1178 ± 40 Ma indicated by three analyses from 112135. As with sample 112135, the analyses of Group 2 are here interpreted to be of xenocryst zircons, possibly derived from the source rocks of the precursor granites. The date of 1005 ± 46 Ma indicated by the analyses of Group 3 is within error of the date of 1016 ± 10 Ma indicated by two analyses from sample 112135. These analyses are interpreted to be from sites that have lost some radiogenic Pb during a disturbance event at this time. The $^{207}\text{Pb}/^{206}\text{Pb}$ date of 531 ± 64 Ma indicated by concordant analysis 17.1 is within error of the time of intrusion of granitic rocks within the Leeuwin Complex (see results for 112140, 112144A, and 112145 documented herein). The low thorium content indicated by this analysis suggests that the zircon rim at this analysis site may have formed during a metamorphic event. Alternatively, the analysis site may have lost all of its accumulated radiogenic Pb during a metamorphic event at this time.

Locality 12: Biotite–hornblende monzogranite dyke, Gracetown

Along the coast about 1 km south of Gracetown and at the end of the main path from the car park (AMG 313200E 6249600N), an approximately 1 m-thick, dark-grey, fine-grained vertical granite dyke has intruded at a high angle to the foliation into a pink, medium-grained hornblende granite gneiss. The foliation in the gneiss has been deformed into open folds, and lenses of amphibolite are present. The dyke is even-grained, unfoliated, and contains oligoclase, quartz, and microcline, with lesser biotite and green hornblende, minor titanite and metamict allanite, and accessory opaques, zircon, apatite, and secondary calcite. Microcline forms subhedral crystals up to 2 mm across, often sieved with small blebs of quartz, and possibly originating from a granophyric intergrowth. Biotite and hornblende are commonly associated, with biotite replacing hornblende in part. The titanite is colourless and forms large masses up to 1.5 mm across. Metamict allanite forms crystals up to 1 mm across. The texture of the rock is essentially igneous, and metamorphism has been at low grade. The original rock was probably a mafic-rich monzogranite. A geochemical analysis of a sample taken from the dyke (112140) is given in Table 1.

Colourless to light green-yellow, euhedral to subhedral zircons averaging 150×250 μm in size were extracted from the dyke. Igneous zonation could be seen in many crystals, whereas others lacked obvious internal structure. Extensive irregular pitting (possibly resulting during the polishing process) of metamict zones or melt inclusions incorporated into the crystals was evident in most grains. Fluid inclusions were common. Twenty analyses were obtained on 19 zircons. Results are shown on a concordia plot in Figure 13. Eighteen analyses have $^{206}\text{Pb}/^{238}\text{U}$ ratios almost within error of a single value (chi-squared = 1.29) corresponding to an weighted mean $^{206}\text{Pb}/^{238}\text{U}$ date of 524 ± 12 Ma. This is interpreted as the time of crystallization of the monzogranite dyke. The weighted mean $^{207}\text{Pb}/^{235}\text{U}$ date is analytically indistinguishable (517 ± 12 Ma, chi-squared = 0.95) from the $^{206}\text{Pb}/^{238}\text{U}$ date, thus indicating that the population is concordant. The weighted mean $^{207}\text{Pb}/^{206}\text{Pb}$ date is 505 ± 25 Ma. Analysis 9.1 has a $^{206}\text{Pb}/^{238}\text{U}$ date of 699 ± 17 Ma (1 σ error); this grain is probably a xenocryst. Analysis 7.1 has a $^{206}\text{Pb}/^{238}\text{U}$ date of 487 ± 12 Ma (1 σ error), slightly lower than that

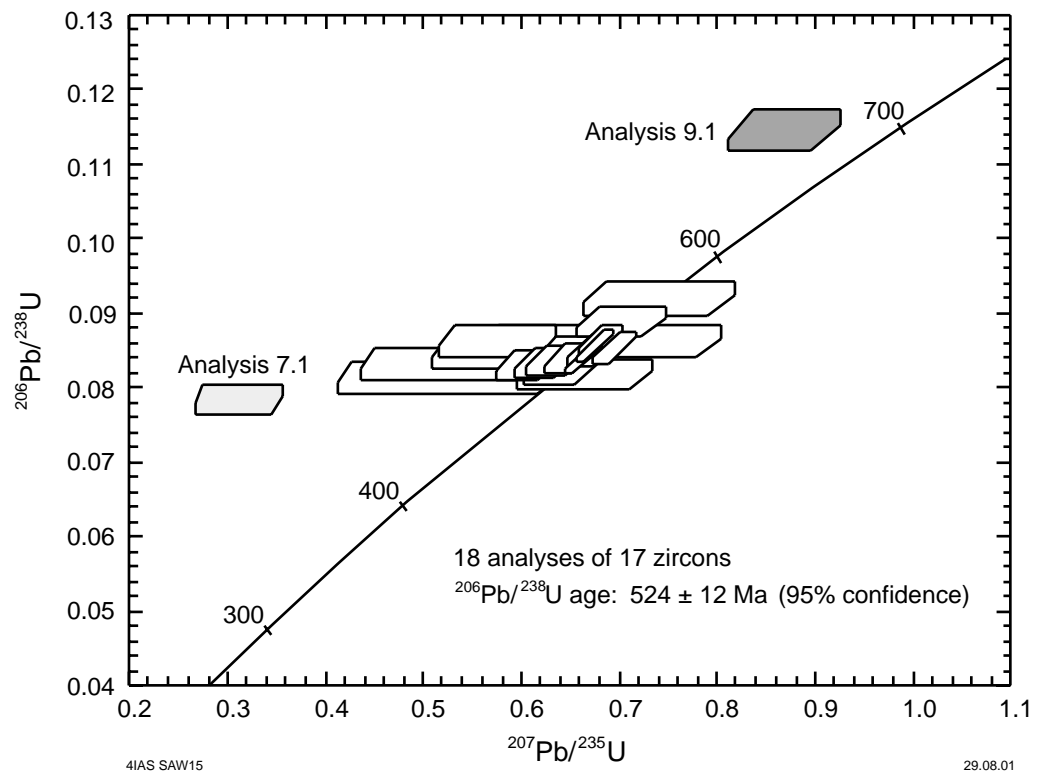


Figure 13. Concordia diagram for 112140: monzogranite dyke, Gracetown

of the main population, either because an inappropriate common Pb composition has been assumed or because of disturbance.

Locality 13: Hornblende–biotite granite gneiss, Cowaramup Bay North

Granite gneiss, metagabbro, and anorthosite are present along the coast about 1 km north of Cowaramup Bay (AMG 313800E 6252200N). Many of the Leeuwin Complex gneisses seen so far have a steeply dipping, north-trending foliation. However, as with the gneisses at Redgate Beach, gneisses at this locality have a weak, subhorizontal foliation and weather to form large blocky tors. A sample of the gneiss (112143) was processed for SHRIMP U–Pb zircon dating. This sample consisted of a medium-grained mosaic of quartz, oligoclase, and microcline, with minor hornblende, opaques, and biotite, and accessory muscovite, apatite, titanite, and zircon. The average grain size is less than 1 mm and the mineral orientation is negligible, but there is some layering of the felsic minerals. Plagioclase twinning is poorly developed or absent; the untwinned plagioclase is commonly antiperthitic and contains small blebs of microcline. The hornblende is an olive green-brown variety, and the biotite is a red-brown titaniferous variety. The original rock was an iron-rich monzogranite and metamorphism was medium grade.

The zircons extracted from this sample were typically colourless to light green-yellow, euhedral to subhedral, and averaged $60 \times 100 \mu\text{m}$ in size. Igneous zonation could be seen in some crystals, but most lacked obvious internal structure. Nineteen analyses were obtained on 19 zircons. Results are shown on a concordia plot in Figure 14. All analyses have $^{206}\text{Pb}/^{238}\text{U}$ ratios almost within error of a single value

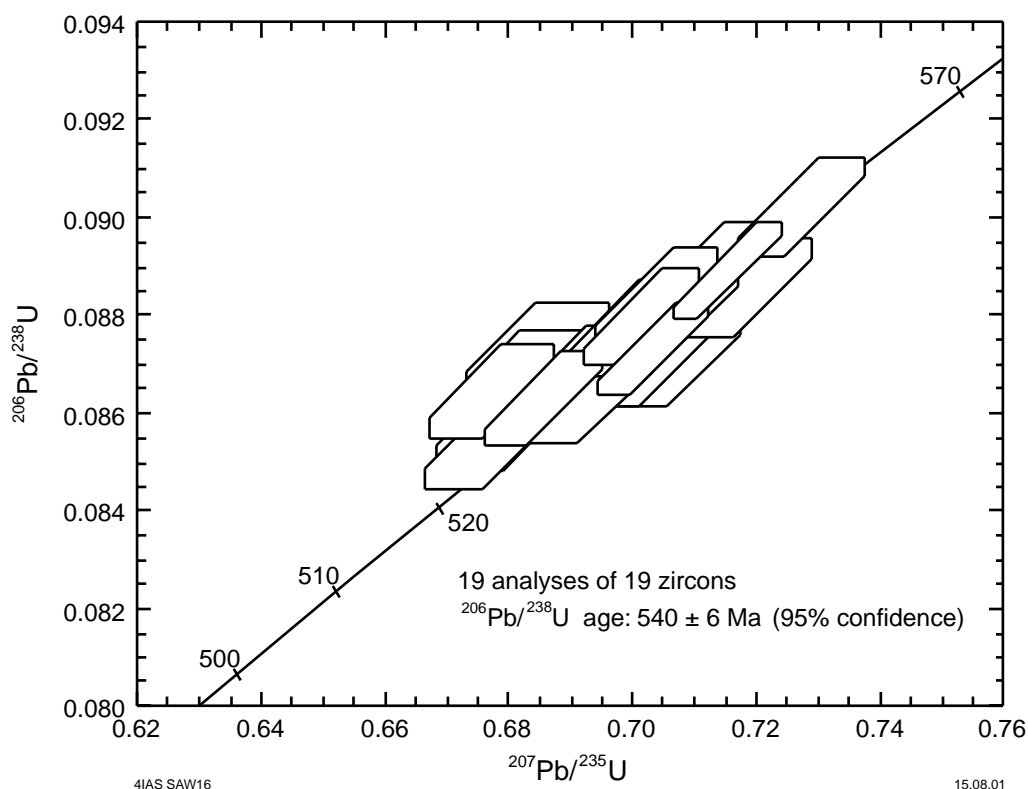


Figure 14. Concordia diagram for 112143: monzogranite gneiss, Cowaramup Bay North

(chi-squared = 1.46) and corresponding to an weighted mean $^{206}\text{Pb}/^{238}\text{U}$ date of 540 ± 6 Ma. This is interpreted as the best estimate of the time of crystallization of the monzogranite precursor to the gneiss. The weighted mean $^{207}\text{Pb}/^{235}\text{U}$ date is analytically indistinguishable (538 ± 5 Ma, chi-squared = 1.94) from the $^{206}\text{Pb}/^{238}\text{U}$ date, thus indicating that the population is concordant. The weighted mean $^{207}\text{Pb}/^{206}\text{Pb}$ date is 532 ± 10 Ma.

Locality 14: Hornblende–biotite granite gneiss, Canal Rocks North

A coarse porphyroclastic (augen) granite gneiss is present on the headland south of Smiths Beach (AMG 315500E 6273700N). Geochemical data on a sample (112144A) of this gneiss are listed in Table 1. The rock is a medium- to coarse-grained (0.5–4 mm), moderately foliated granoblastic gneiss containing perthite, quartz, hornblende, and plagioclase, with accessory biotite, opaques, apatite, and zircon. Plagioclase is present mostly as untwinned albite in large patches of myrmekitic intergrowth. The hornblende is a dark olive-green hastingsitic variety with low 2V. The original rock was granitic and metamorphism was medium grade.

The zircons extracted from this sample were typically colourless to light-golden yellow, euhedral to subhedral, and averaged 200–450 μm in size. Igneous zonation and small fluid and opaque inclusions could be seen in most crystals. Twenty-three analyses were obtained on 23 zircons. Results are shown on a concordia plot in Figure 15. All analyses can be assigned to four groups. Group 1, consisting of 14 analyses, has $^{206}\text{Pb}/^{238}\text{U}$ ratios indicating some excess scatter (chi-squared = 2.10) and corresponding to a weighted mean $^{206}\text{Pb}/^{238}\text{U}$ date of 702 ± 7 Ma. For Group 1 analyses, the weighted mean $^{207}\text{Pb}/^{235}\text{U}$ date is analytically indistinguishable (705 ± 8 Ma, chi-squared = 2.01)

from the $^{206}\text{Pb}/^{238}\text{U}$ date, thus indicating that the population is concordant, and the weighted mean $^{207}\text{Pb}/^{206}\text{Pb}$ date is 721 ± 23 Ma. The $^{206}\text{Pb}/^{238}\text{U}$ date of Group 1 analyses is interpreted as the best estimate of the time of crystallization of the monzogranite precursor to the gneiss. Group 3, consisting of four analyses, has $^{206}\text{Pb}/^{238}\text{U}$ ratios indicating a small amount of excess scatter (chi-squared = 1.50) and corresponding to a weighted mean $^{206}\text{Pb}/^{238}\text{U}$ date of 625 ± 14 Ma. The $^{207}\text{Pb}/^{235}\text{U}$ date is 634 ± 30 Ma (chi-squared = 1.94). Group 3 analyses may give the time of a metamorphic disturbance event. The four analyses assigned to Group 2 are interpreted to be of sites consisting of both Group 1 and 3 components. Analysis 2.1 has a $^{206}\text{Pb}/^{238}\text{U}$ date of 560 ± 6 Ma and a $^{207}\text{Pb}/^{235}\text{U}$ date of 561 ± 12 Ma (1σ error).

Locality 15: Aegirine-augite-quartz syenite gneiss, Gannet Rock

Aegirine-augite-quartz syenite is present along the north coast of the Leeuwin Complex. A sample of this gneiss (112145) was taken from Gannet Rock (AMG 322400E 6283900N), west of Meelup Beach. The sample is of a fine to medium, even-grained, pink granitic gneiss consisting of microcline, albite, quartz, minor aegirine-augite and opaques, and accessory titanite, amphibole, zircon, and apatite. Secondary calcite is also present. The feldspar is an unmixed perthite consisting of small grains of albite enclosed in microcline (or vice versa), and relict grains of perthite. The original grain size was 2 to 3 mm, but the neoblasts are generally less than 0.5 mm. Small grains of bright-green aegirine-augite are partially altered to actinolite or chlorite. The proportion of quartz is low and the rock is borderline between granite and quartz syenite. Metamorphic grade is indeterminate, but probably low.

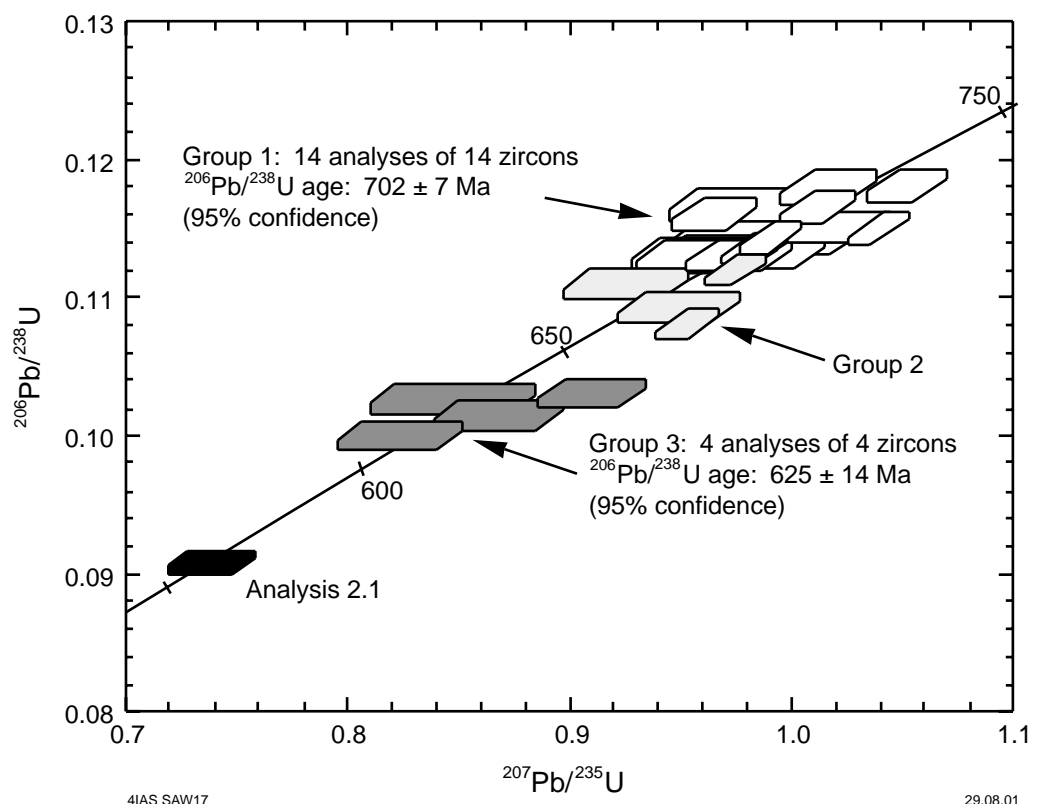


Figure 15. Concordia diagram for 112144A: monzogranite gneiss, Canal Rocks North

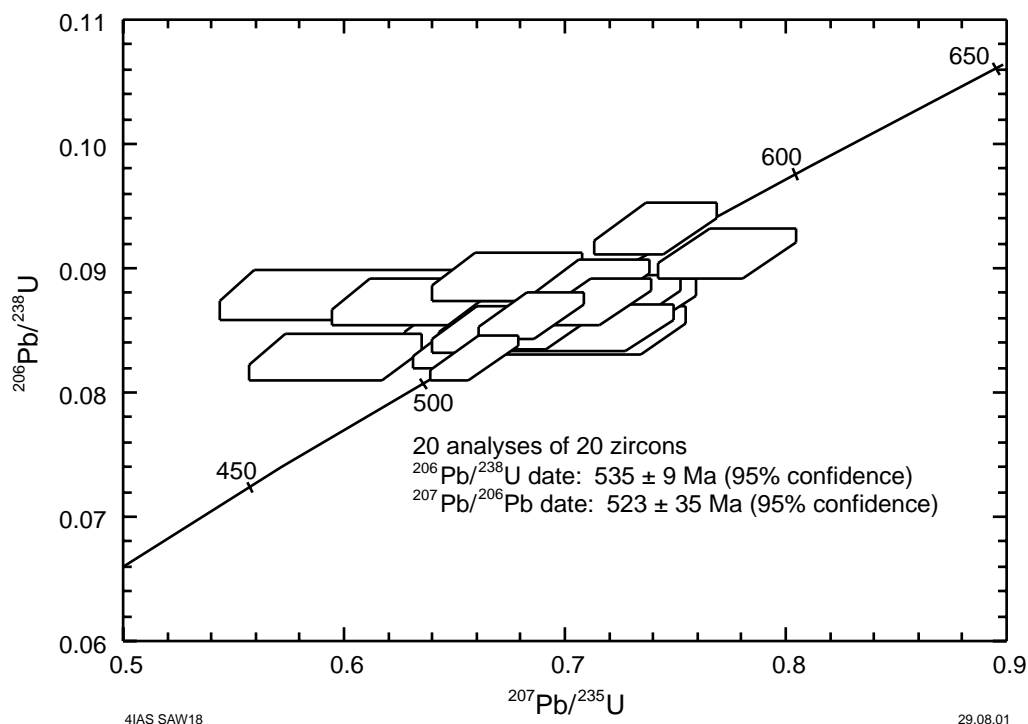


Figure 16. Concordia diagram for 112145: gneiss, Gannet Rock

The zircons isolated from this sample are commonly colourless to pale green-yellow, elongate, subhedral with rounded terminations, and between $40 \times 100 \mu\text{m}$ and $12 \times 450 \mu\text{m}$ in size. Many grains are structureless, although a minority of grains have small rounded cores, or fluid or opaque mineral inclusions, or both. Twenty analyses were obtained from 20 zircons. Results are shown on a concordia plot in Figure 16. All analyses are concordant and have $^{207}\text{Pb}/^{206}\text{Pb}$ ratios defining a single population and indicating a weighted mean $^{207}\text{Pb}/^{206}\text{Pb}$ date of $523 \pm 35 \text{ Ma}$ (chi-squared = 0.87). The weighted mean $^{207}\text{Pb}/^{235}\text{U}$ date is $532 \pm 12 \text{ Ma}$ (chi-squared = 1.36) and the weighted mean $^{206}\text{Pb}/^{238}\text{U}$ date is $535 \pm 9 \text{ Ma}$ (chi-squared = 1.69). This is interpreted as the time of igneous crystallization of the granitic precursor to the gneiss.

Locality 16: Bunker Bay

Gneissic rocks of the Leeuwin Complex are overlain by the Tamala Limestone, a Quaternary calcareous dune system extensively developed along the coast of Western Australia. At this locality, there is a marked angular unconformity, the base of which is marked by conglomerate. The gneisses range from hornblende to granodiorite in composition, with the mineralogy dominated by plagioclase, hornblende, clinopyroxene, garnet, and biotite. The general foliation trend is westerly to northwesterly, with a shallow northerly dip of 30° . A prominent mineral lineation plunges north at 30° and there are rare isoclinal folds parallel to this. The more mafic bands are commonly boudinaged approximately perpendicular to the lineation. These gneisses are crosscut and injected parallel to the layering by a pink pegmatitic granite that post-dates the main fabric development. This granite phase may be related to the Meelup granite of Myers (1994).

Locality 17: Bunbury Basalt

To close our brief overview of the geological evolution of southwestern Australia, we visit the Bunbury Basalt on the foreshore just south of the Bunbury lighthouse. The basalt consists of two main lava flows separated by a thin layer of sediments that include basaltic detritus. These two pulses of magmatism have been dated at 130 and 123 Ma respectively (Frey et al., 1996). The basalt is porphyritic, with prominent plagioclase phenocrysts, and is locally vesicular. It also shows excellent columnar jointing. The basalt was extruded subaerially and appears to infill valleys eroded into the Jurassic Yarragadee Formation on both sides of the Darling Fault. Kent (1991) has suggested that the Bunbury Basalt may be a reflection of the Kerguelen plume and that this was possibly a hot spot beneath Eastern Gondwanaland prior to continental breakup. However, doubt has been cast on this view (Müller et al., 1993), since it may have been erupted up to 1000 km from the plume.

Acknowledgements

Much of the work undertaken by Simon Wilde was initially conducted whilst he was a member of the Geological Survey of Western Australia. Subsequent work was supported by the Australian Research Council and Curtin University of Technology.

The work undertaken by David Nelson is published with permission of the Director, GSWA. Thin section preparation and the processing of samples to extract zircon for SHRIMP U–Pb dating was undertaken by John Williams and the technical staff of the GSWA Carlisle Laboratories. Petrographic descriptions in this report were made by J. Lewis (formerly GSWA).

References

- ARRIENS, P. A., 1971, The Archaean geochronology of Australia: Geological Society of Australia, Special Publication no. 3, p. 11–23.
- BATCHELOR, R. A., and BOWDEN, P., 1985, Petrogenetic interpretation of granitoid rock series using multicantionic parameters: *Chemical Geology*, v. 48, p. 43–55.
- BAXTER, J. L., and LIPPLE, S. L., 1985, Perenjori, W.A.: Western Australia Geological Survey, 1:250 000 Geological Series Explanatory Notes, 32p.
- BEESON, J., DELOR, C. P., and HARRIS, L. B., 1988, A structural and metamorphic traverse across the Albany Mobile Belt, Western Australia: *Precambrian Research*, v. 40/41, p. 117–136.
- BLACK, L. P., SHERATON, J. W., TINGEY, R. J., and McCULLOCH, M. T., 1992, New U–Pb zircon ages from the Denman Glacier area, East Antarctica, and their significance for Gondwana reconstruction: *Antarctic Science*, v. 4, p. 447–460.
- BLIGHT, D. F., COMPSTON, W., and WILDE, S. A., 1981, The Logue Brook Granite: age and significance of deformation zones along the Darling Scarp: Western Australia Geological Survey, Annual Report for 1980, p. 72–80.
- BONIN, B., 1990, From orogenic to anorogenic settings: Evolution of granitoid suites after a major orogenesis: *Geological Journal*, v. 25, p. 261–270.
- BRETAN, P. G., 1985, Deformation processes within mylonite zones associated with some fundamental faults: University of London, PhD thesis (unpublished).
- BRUGUIER, O., BOSCH, D., PIDGEON, R. T., BYRNE, D. I., and HARRIS, L. B., 1999, U–Pb chronology of the Northampton Complex, Western Australia — evidence for Grenvillian sedimentation, metamorphism and deformation and geodynamic implications: *Contributions to Mineralogy and Petrology*, v. 136, p. 258–272.
- BURGESS, A. I. R., 1978, Geology and geochemistry of the Cretaceous Bunbury Basalt: University of Western Australia, Hons thesis (unpublished).
- CAMPBELL, I. H., and HILL, R. I., 1988, A two-stage model for the formation of the granite–greenstone terrains of the Kalgoorlie–Norseman area, Western Australia: *Earth and Planetary Science Letters*, v. 90, p. 11–25.
- CLEMENS, J. D., HOLLAWAY, J. R., and WHITE, A. J. R., 1986, Origins of an A-type granite: experimental constraints: *American Mineralogist*, v. 71, p. 317–324.
- COBB, M., 2000, Age and origin of the Mullingar Complex and its role in East Gondwana: Western Australia, Curtin University of Technology, Applied Geology Hons thesis (unpublished).
- COBB, M. M., CAWOOD, P. A., KINNY, P. D., and FITZSIMONS, I. C. W., 2001, SHRIMP U–Pb zircon ages from the Mullingar Complex, Western Australia: isotopic evidence for allochthonous blocks in the Pinjarra Orogen and implications for East Gondwana assembly: *Geological Society of Australia, Abstracts*, v. 64, p. 21–22.
- COMPSTON, W., and ARRIENS, P. E., 1968, The Precambrian geochronology of Australia: *Canadian Journal of Geological Sciences*, v. 5, p. 561–583.
- COMPSTON, W., WILLIAMS, I. S., and McCULLOCH, M. T., 1986, Contrasting zircon U–Pb and model Sm–Nd ages from the Archaean Logue Brook Granite: *Australian Journal of Earth Sciences*, v. 33, p. 193–200.
- COMPSTON, W., WILLIAMS, I. S., CAMPBELL, I. H., and GRESHAM, J. J., 1985, Zircon xenocrysts from the Kambalda volcanics: age constraints and direct evidence for older continental crust below the Kambalda–Norseman greenstones: *Earth and Planetary Science Letters*, v. 76, p. 299–311.
- CREASER, R. A., PRICE, R. C., and WORMALD, R. J., 1991, A-type granites revisited: assessment of a residual-source model: *Geology*, v. 19, p. 163–166.
- DALZIEL, I. W. D., 1991, Pacific margins of Laurentia and East Antarctica – Australia as a conjugate rift pair: evidence and implications for an Eocambrian supercontinent: *Geology*, v. 19, p. 598–601.
- de LAETER, J. R., and LIBBY, W. G., 1993, Early Palaeozoic biotite Rb–Sr dates in the Yilgarn Craton near Harvey, Western Australia: *Australian Journal of Earth Sciences*, v. 40, p. 445–453.
- EBY, G. N., 1992, Chemical subdivision of the A-type granitoids: Petrogenetic and tectonic implications: *Geology*, v. 20, p. 641–644.
- FAIRBRIDGE, R. W., and FINKL, C. W. Jr., 1978, Geomorphic analysis of the rifted cratonic margins of Western Australia: *Zeitschrift für Geomorphologie N.F.*, v. 22, p. 369–389.
- FALVEY, D. A. 1972, Sea-floor spreading in the Wharton Basin (northeast Indian Ocean) and the breakup of eastern Gondwanaland: *Australian Petroleum Exploration Association Journal*, v. 12, p. 86–88.
- FITZSIMONS, I. C. W., COBB, M. M., CAWOOD, P. A., and KINNY, P. D., 2001, Proterozoic accretion and reactivation along the Darling Mobile Belt of Western Australia: *Geological Society of Australia, Abstracts*, v. 64, p. 44–45.
- FLETCHER, I. R., and LIBBY, W. G., 1993, Further isotopic evidence for the existence of two distinct terranes in the southern Pinjarra Orogen, Western Australia: Western Australia Geological Survey, Report 37, p. 81–83.
- FLETCHER, I. R., LIBBY, W. G., and ROSMAN, K. J. R., 1987, Geological Note: Sm–Nd dating of the 2411 Ma Jimberlana dyke, Yilgarn Block, Western Australia: *Australian Journal of Earth Sciences*, v. 34, p. 523–525.

- FLETCHER, I. R., WILDE, S. A., LIBBY, W. G., and ROSMAN, K. J. R., 1983a, Sm–Nd model ages across the margins of the Archaean Yilgarn Block, Western Australia — II; Southwest transect into the Proterozoic Albany–Fraser Province: *Geological Society of Australia, Journal*, v. 30, p. 333–340.
- FLETCHER, I. R., WILDE, S. A., and ROSMAN, K. J. R., 1985, Sm–Nd ages across the margins of the Archaean Yilgarn Block, Western Australia — III; the Western margin: *Australian Journal of Earth Sciences*, v. 32, p. 73–82.
- FLETCHER, I. R., WILLIAMS, S. J., GEE, R. D., and ROSMAN, K. J. R., 1983b, Sm–Nd model ages across the margins of the Archaean Yilgarn Block, Western Australia; northwest transect into the Proterozoic Gascoyne Province: *Geological Society of Australia, Journal*, v. 30, p. 167–174.
- FREY, F. A., McNAUGHTON, N. J., NELSON, D. R., de LAETER, J. R., and DUNCAN, R. A., 1996, Petrogenesis of the Bunbury Basalt, Western Australia: interaction between the Kerguelen plume and Gondwana lithosphere?: *Earth and Planetary Science Letters*, v. 144, p. 163–183.
- FROST, C. D., SCOATES, J. S., CHAMBERLAIN, K. R., and EDWARDS, B. R., 1994, Two mechanisms of granite formation, Laramie Anorthosite Complex, Wyoming, ICOG-8 Abstract: United States Geological Survey, Circular 1107, p. 106.
- GEE, R. D., 1979, Structure and tectonic style of the Western Australian Shield: *Tectonophysics*, v. 58, p. 327–369.
- GEE, R. D., BAXTER, J. L., WILDE, S. A., and WILLIAMS, I. R., 1981, Crustal development in the Archaean Yilgarn Block, Western Australia: *Geological Society of Australia, Special Publication no. 7*, p. 43–56.
- GIDDINGS, J. W., 1976, Precambrian palaeomagnetism in Australia 1: Basic dykes and volcanics from the Yilgarn Block: *Tectonophysics*, v. 30, p. 91–108.
- GLIKSON, A. Y., and LAMBERT, I. B., 1976, Vertical zonation and petrogenesis of the early Precambrian crust in Western Australia: *Tectonophysics*, v. 30, p. 55–89.
- HARRIS, L. B., 1987, A tectonic framework for the Western Australian Shield and its significance to gold mineralisation, *in* Recent advances in the understanding of Precambrian gold deposits *edited by* S. HO and D. I. GROVES: University of Western Australia, Department of Geology and Extension Service, Publication no. 11, p. 1–27.
- HENSEN, B. J., and ZHOU, B., 1995, A Pan-African granulite facies metamorphic episode in Prydz Bay, Antarctica: evidence from Sm–Nd garnet dating: *Australian Journal of Earth Sciences*, v. 42, p. 249–258.
- HOCKING, R. M., 1994, Subdivisions of Western Australian Neoproterozoic and Phanerozoic sedimentary basins: Western Australia Geological Survey, Record 1994/4, 84p.
- KENT, R. W., 1991, Lithospheric uplift in eastern Gondwana: evidence from a long-lived mantle plume system?: *Geology*, v. 19, p. 19–23.
- KENT, R. W., STOREY, M., and SAUNDERS, A. O., 1992, Large igneous provinces: sites of plume impact or plume incubation?: *Geology*, v. 20, p. 891–894.
- LIBBY, W. G., and de LAETER, J. R. 1979, Biotite dates and cooling history at the western margin of the Yilgarn Block: Western Australia Geological Survey, Annual Report for 1978, p. 79–87.
- LIBBY, W. G., de LAETER, J. R., and ARMSTRONG, R. A., 1999, Proterozoic biotite Rb–Sr dates in the northwestern part of the Yilgarn Craton, Western Australia: *Australian Journal of Earth Sciences*, v. 46, p. 851–860.
- LOISELLE, M. C., and WONES, D. R., 1979, Characteristics and origin of anorogenic granites: *Geological Society of America, Abstracts* 11, 468p.
- LOW, G. H., 1975, Proterozoic rocks on or adjoining the Yilgarn Block, *in* The Geology of Western Australia: Western Australia Geological Survey, Memoir 2, p. 71–81.
- McCULLOCH, M. T., 1987, Sm–Nd isotopic constraints on the evolution of Precambrian crust in the Australian continent, *in* Proterozoic lithospheric evolution (Geodynamics series 17) *edited by* A. KRONER: American Geophysical Union and Geological Society of America International Lithospheric Program, Publication 0130, p. 115–130.
- McLELLAND, J., ASHWALL, L., and MOORE, L., 1994, Composition and petrogenesis of oxide-, apatite-rich gabbro-norites associated with Proterozoic anorthosite massifs: examples from the Adirondack Mountains, New York: *Contributions to Mineralogy and Petrology*, v. 116, p. 225–238.
- MIDDLETON, M. F., WILDE, S. A., EVANS, B. J., LONG, A., DENTITH, M., and MORAWA, M. A., 1995, Implications of a geoscientific traverse over the Darling Fault Zone, Western Australia: *Australian Journal of Earth Sciences*, v. 42, p. 83–93.
- MÜLLER, R. D., ROYER, J.-V., and LAWVER, L. A., 1993, Revised plate motions relative to hotspots from combined Atlantic and Indian Ocean hotspot tracks: *Geology*, v. 21, p. 275–278.
- MYERS, J. S., 1990, Anorthosite in the Leeuwin Complex of the Pinjarra Orogen, Western Australia: *Australian Journal of Earth Sciences*, v. 37, p. 241–245.
- MYERS, J. S., 1993, Precambrian history of the West Australian craton and adjacent orogens: *Annual Review of Earth and Planetary Sciences*, v. 21, p. 453–485.
- MYERS, J. S., 1994, Late Proterozoic high-grade gneiss complex between Cape Leeuwin and Cape Naturaliste: Geological Society of Australia (WA Division), Excursion Guidebook 6, 26p.
- MYERS, J. S., SHAW, R. D., and TYLER, I. M., 1996, Tectonic evolution of Proterozoic Australia: *Tectonics*, v. 15, p. 1431–1446.

- NELSON, D. R. 1995, Field Guide to the Leeuwin Complex, Western Australia: Australian Conference on Geochronology and Isotope Science 3, Perth, 1995, Special Publication, 24p.
- NELSON, D. R., 1999, Compilation of geochronology data, 1998: Western Australia Geological Survey, Record 1999/2, 222p.
- NELSON, D. R., MYERS, J. S., and NUTMAN, A. P., 1995, Chronology and evolution of the Middle Proterozoic Albany–Fraser Orogen, Western Australia: Australian Journal of Earth Sciences, v. 42, p. 481–495.
- NEMCHIN, A. A., and PIDGEON, R. T., 1997, Evolution of the Darling Range Batholith, Yilgarn Craton, Western Australia: Journal of Petrology, v. 38, p. 625–649.
- NIEUWLAND, D. A., 1980, Structural geology and geochronology of the Toodyay district, Western Australia: Australian National University, PhD thesis (unpublished).
- NIEUWLAND, D. A., and COMPSTON, W., 1981, Crustal evolution in the Yilgarn Block near Perth, Western Australia: Geological Society of Australia, Special Publication no. 7, p. 159–171.
- OLIVER, R. L., COOPER, J. A., and TRUELOVE, A. J., 1983, Petrology and zircon geochronology of Herring Island and Commonwealth Bay and evidence for Gondwana reconstruction, in Antarctic Earth Science *edited by* R. L. OLIVER, P. R. JAMES, and J. B. JAGO: Canberra, Australian Academy of Science, p. 64–68.
- PARTINGTON, G. A., 1990, Geology of the southwestern Yilgarn and Greenbushes Pegmatite Group, in Third International Archaean Symposium, Perth, 1990, Excursion Guidebook *edited by* S. E. HO, J. E. GLOVER, J. S. MYERS, and J. R. MUHLING: University of Western Australia, Department of Geology and Extension Service, Publication no. 21, p. 123–144.
- PARTINGTON, G. A., McNAUGHTON, N. J., KEPERT, D. A., COMPSTON, W., and WILLIAMS, I. S., 1986, Geochronology of the Balingup Metamorphic Belt: constraints on the temporal evolution of the Greenbushes Pegmatite District: Australia Bureau of Mineral Resources, Record 1986/10, p. 55–56.
- PEARCE, J. A., HARRIS, N. B. W., and TINDLE, A. G., 1984, Trace element discrimination diagrams for the tectonic discrimination of granitic rocks: Journal of Petrology, v. 25, p. 956–983.
- PEERS, R., 1975, Northampton Block, in The Geology of Western Australia: Western Australia Geological Survey, Memoir 2, p. 104–106.
- PITCHER, W. S., 1993, The Nature and Origin of Granite: Chapman and Hall, London, 387p.
- PLAYFORD, P. E., COCKBAIN, A. E., and LOW, G. H., 1976, Geology of the Perth Basin, Western Australia: Western Australia Geological Survey, Bulletin 124, 311p.
- PLAYFORD, P. E., COPE, R. N., COCKBAIN, A. E., LOW, G. H., and LOWRY, D. C., 1975, Phanerozoic, in The Geology of Western Australia: Western Australia Geological Survey, Memoir 2, p. 223–433.
- POWELL, C. McA., ROOTS, S. R., and VEEVERS, J. J., 1988, Pre-breakup continental extension in East Gondwanaland and the early opening of the eastern Indian Ocean: Tectonophysics, v. 155, p. 261–283.
- PRINGLE, M. S., STOREY, M., and WIJBRANS, J., 1994, $^{40}\text{Ar}/^{39}\text{Ar}$ geochronology of mid-Cretaceous Indian Ocean basalts: constraints on the origin of large flood basalt provinces: Eos, Transactions of American Geophysical Union, v. 75, 728p.
- ROSMAN, K. J. R., WILDE, S. A., LIBBY, W. G., and de LAETER, J. R., 1980, Rb–Sr dating of granitic rocks in the Pemberton area: Western Australia Geological Survey, Annual Report for 1979, p. 97–100.
- SARKAR, A. N., BHANUMATHI, L., and BALASUBRAHMANYAN, M. N., 1981, Petrology, geochemistry and geochronology of the Chilka Lake igneous complex, Orissa State, India: Lithos, v. 14, p. 93–111.
- SHIRAIISHI, K., ELLIS, D. J., HIROI, Y., FANNING, M., MOTOYOSHI, Y., and NAKAI, Y., 1994, Cambrian orogenic belt in East Antarctica and Sri Lanka: implications for Gondwana assembly: Journal of Geology, v. 102, p. 47–65.
- SYLVESTER, P. J., 1989, Post-collisional alkaline granites: Journal of Geology, v. 97, p. 261–280.
- TINGEY, R. J., 1991, The regional geology of Archaean and Proterozoic rocks in Antarctica, in The Geology of Antarctica *edited by* R. J. TINGEY: Oxford, Oxford University Press, p. 1–73.
- TORSVIK, T. H., SMETHURST, M. A., MEERT, J. G., VAN DER VOO, R., McKERROW, W. S., BRASIER, M. D., STURT, B. A., and WALDERHAUG, H. J., 1996, Continental break-up and collision in the Neoproterozoic and Paleozoic — A tale of Baltica and Laurentia: Earth Science Reviews, v. 40, p. 229–258.
- UNNIKRISHNAN-WARRIER, C., YOSHIDA, M., KAGAMI, H., and SANTOSH, M., 1993, Geochronological constraints on granulite formation in southern India: implications for east Gondwana reassembly: Osaka City University, Journal of Geosciences, v. 36(5), p. 109–121.
- VEEVERS, J. J., 1984, Morphotectonics of the divergent or rifted margins, in Phanerozoic Earth History of Australia *edited by* J. J. VEEVERS: Oxford, Clarendon Press, Oxford Monographs on Geology and Geophysics, no. 2, p. 168–210.
- VEEVERS, J. J., and COTTERILL, D., 1978, Western margin of Australia, evolution of a rifted arch system: Geological Society of America, Bulletin 89, p. 337–355.
- VEEVERS, J. J., and LI, Z. X., 1991, Review of seafloor spreading around Australia: II, marine magnetic anomaly modelling: Australian Journal of Earth Sciences, v. 38, p. 391–408.
- VEEVERS, J. J., POWELL, C. McA., and ROOTS, S. R., 1991, Review of seafloor spreading around Australia. I: synthesis of the patterns of spreading: Australian Journal of Earth Sciences, v. 38, p. 373–389.

- WHALEN, J. B., CURRIE, K. L., and CHAPPELL, B. W., 1987, A-type granites: geochemical characteristics, discrimination and petrogenesis: *Contributions to Mineralogy and Petrology*, v. 95, p. 407–419.
- WHALEN, J. B., JENNER, G. A., LONGSTAFFE, F. J., ROBERT, F., and GARIEPY, C., 1996, Geochemical and isotopic (O, Nd, Pb and Sr) constraints on A-type granite petrogenesis based on the Topsails Igneous Suite, Newfoundland, Appalachians: *Journal of Petrology*, v. 37, p. 1463–1489.
- WHITECHURCH, H., MONTIGNY, R., SEVIGNY, J., STOREY, M., and SALTERS, V., 1992, K–Ar and ^{40}Ar – ^{39}Ar ages of central Kerguelen Plateau basalts: *Proceedings of Ocean Drilling Program, Scientific Results* 120, p. 71–77.
- WILDE, S. A., 1980, The Jimpending Metamorphic Belt in the Toodyay area and the Balingup Metamorphic Belt and associated granitic rocks of the Southwestern Yilgarn Block: *International Archaean Symposium*, 2nd, Perth 1980: Geological Society of Australia, Excursion Guide, 41p.
- WILDE, S. A., 1981, A brief review of the geology of Southwestern Australia, *in* *Mineral Fields of the Southwest, Western Australia* edited by T. E. JOHNSTON: Geological Society of Australia, 5th Geological Convention, Perth, Field Excursion Guidebook, p. 2–21.
- WILDE, S. A., 1990, Geology and crustal evolution of the southwestern Yilgarn Craton, *in* *Third International Archaean Symposium*, Perth, 1990, Excursion Guidebook edited by S. E. HO, J. E. GLOVER, J. S. MYERS, and J. R. MUHLING: University of Western Australia, Department of Geology and Extension Service, Publication, no. 21, p. 97–122.
- WILDE, S. A., 2000, Evolution of the western margin of Australia during the Rodinian and Gondwanan Supercontinent Cycles: *Gondwana Research*, v. 2, p. 481–499.
- WILDE, S. A., and LOW, G. H., 1978, Perth, W.A.: Western Australia Geological Survey, 1:250 000 Geological Series Explanatory Notes, 36p.
- WILDE, S. A., MIDDLETON, M. F., and EVANS, B. J., 1996, Terrane accretion in the southwest Yilgarn Craton: evidence from a deep seismic crustal profile: *Precambrian Research*, v. 78, p. 179–196.
- WILDE, S. A., and MURPHY, D. M. K., 1990, The nature and origin of the Late Proterozoic high-grade gneisses of the Leeuwin Block, Western Australia: *Precambrian Research*, v. 47, p. 251–270.
- WILDE, S. A., and WALKER, I. W., 1982, Collie, W.A.: Western Australia Geological Survey, 1:250 000 Geological Series Explanatory Notes, 39p.
- WILDE, S. A., and WALKER, I. W., 1984, Pemberton–Irwin Inlet, W.A.: Western Australia Geological Survey, 1:250 000 Geological Series Explanatory Notes, 37p.
- WILSON, A. F., 1958, Advances in the knowledge of the structure and petrology of the Precambrian rocks of southwestern Australia: *Royal Society of Western Australia, Journal*, v. 41, p. 57–83.
- WILSON, A. F., COMPSTON, W., JEFFREY, P. M., and RILEY, G. H., 1960, Radioactive ages from the Precambrian rocks of Australia: *Geological Society of Australia, Journal*, v. 6, p. 179–195.
- WILSON, A. F., and GREEN, D. C., 1971, The use of oxygen isotopes for geothermometry of Proterozoic and Archaean granulites: *Geological Society of Australia, Special Publication* no. 3, p. 389–400.
- WINGATE, M. T. D. and GIDDINGS, J. W., 2000, Age and palaeomagnetism of the Mundine Well dyke swarm, Western Australia: implications for an Australia–Laurentia connection at 755 Ma: *Precambrian Research*, v. 100, p. 335–357.
- ZHAO, G. C., WILDE, S. A., and CAWOOD, P. A., 2000, Two Pre-Rodinia Supercontinents?: evidence from the reconstruction of global 2.1–1.8 Ga orogens and associated cratons: Brazil, *International Geological Conference*, 31st, Abstracts.